Communications in Analysis and Mechanics

https://www.aimspress.com/journal/cam

Communications in Analysis and Mechanics, 16(1): 24–52.
DOI: 10.3934/cam.2024002
Received: 17 October 2023
Revised: 23 November 2023
Accepted: 02 January 2024
Published: 09 January 2024

Research article

Optimal time two-mesh mixed finite element method for a nonlinear fractional hyperbolic wave model

Yining Yang[1], Cao Wen[1], Yang Liu[1,*], Hong Li[1] and Jinfeng Wang[2]

[1] School of Mathematical Sciences, Inner Mongolia University, Hohhot 010021, China

[2] School of Statistics and Mathematics, Inner Mongolia University of Finance and Economics, Hohhot 010070, China

* **Correspondence:** Email: mathliuyang@imu.edu.cn.

Abstract: In this article, a second-order time discrete algorithm with a shifted parameter θ combined with a fast time two-mesh (TT-M) mixed finite element (MFE) scheme was considered to look for the numerical solution of the nonlinear fractional hyperbolic wave model. The second-order backward difference formula including a shifted parameter θ (BDF2-θ) with the weighted and shifted Grünwald difference (WSGD) approximation for fractional derivative was used to discretize time direction at time $t_{n-\theta}$, the H^1-Galerkin MFE method was applied to approximate the spatial direction, and the fast TT-M method was used to save computing time of the developed MFE system. A priori error estimates for the fully discrete TT-M MFE system were analyzed and proved in detail, where the second-order space-time convergence rate in both L^2-norm and H^1-norm were derived. Detailed numerical algorithms with smooth and weakly regular solutions were provided. Finally, some numerical examples were provided to illustrate the feasibility and effectiveness for our scheme.

Keywords: fractional hyperbolic wave model; time two-mesh mixed finite element method; WSGD operator; error estimates
Mathematics Subject Classification: 65N30, 65M60

1. Introduction

Fractional differential equation models have been founded in a lot of fields of science and engineering, such as physics, chemistry, biology, dynamics, and control [1–4]. In these models, the fractional wave model plays an important role in many practical application fields including transmission and modeling propagation of electrical signals, neural conduction, weak current propagation in the animal nervous system, wave phenomena, and wave propagation. However, it is often difficult to get the analytic solutions of these complex problems. In view of the importance of this kind of model, more and

more scholars have focused on solving them numerically by developing a lot of numerical methods including finite element method [5–14], wavelet method [15], finite difference method [16–23], meshless method [24], collocation method [25, 26], and B-spline method [27, 28].

In this article, we consider the initial-boundary problem of the following nonlinear fractional hyperbolic wave model

$$\begin{cases} {}_0^R D_t^\beta u(x,t) + u_t(x,t) - {}_0^R D_t^\alpha u_{xx}(x,t) - u_{xx}(x,t) + g(u(x,t)) = f(x,t), (x,t) \in \Omega \times J, \\ u(x,0) = u_0(x), u_t(x,0) = u_1(x), x \in \bar{\Omega}, \\ u(a,t) = u(b,t) = 0, u_t(a,t) = u_t(b,t) = 0, t \in J, \end{cases} \tag{1.1}$$

where $\Omega = (a, b)$ is the spatial domain and $J = (0, T]$ with $0 < T < \infty$ is the time interval. $u_0(x)$ and $u_1(x)$ are given initial functions, $f(x, t)$ is the given source term and the nonlinear term $g(u) \in C^2(R)$, fractional parameter $\beta = \alpha + 1$, and ${}_0^R D_t^\gamma w(x,t)$ is the Riemann-Liouville fractional-order derivative defined by

$${}_0^R D_t^\alpha w(x,t) = \frac{1}{\Gamma(1-\alpha)} \frac{\partial}{\partial t} \int_0^t \frac{w(x,s)}{(t-s)^\alpha} ds, \ \alpha \in (0,1), \tag{1.2}$$

and

$${}_0^R D_t^\beta w(x,t) = \frac{1}{\Gamma(2-\beta)} \frac{\partial^2}{\partial t^2} \int_0^t \frac{w(x,s)}{(t-s)^{\beta-1}} ds, \ \beta \in (1,2). \tag{1.3}$$

The fractional hyperbolic wave model (1.1), which includes both propagation and diffusion of the wave, can be degenerated into the pseudo-hyperbolic equation for $\beta = 2$ and diffusion equation for $\beta = 1$.

In the following, for formulating our numerical method we need to introduce numerical techniques including the weighted and shifted Grünwald difference (WSGD) formula, BDF2-θ, H^1-Galerkin MFE method, and time two-mesh (TT-M) finite element algorithm. The WSGD formula, which was proposed by Tian et al. in [29], is a useful approximate method for the Riemann-Liouville fractional derivative. Due to its high-order approximation characteristics, many scholars have developed efficient numerical methods based on the WSGD formula; see [30–35]. The H^1-Galerkin MFE method is an important numerical method, which was proposed by Pani [36]. Due to several advantages of this method, many scholars have begun to use it to solve evolution partial differential equation (PDE) models, such as integer PDE models [37–39], fractional PDE models [40], and distributed-order PDE models [41]. The TT-M finite element method was proposed by Liu et al. in [42] to quickly solve the fractional water wave model, which can also combine many other numerical methods, such as the finite difference method and the finite volume element method, to solve evolution differential equation models [43–46].

In this article, considering the characteristics of the nonlinear fractional hyperbolic wave equation, we introduce an auxiliary function with a fractional derivative, and formulate a fast high-order fully discrete H^1-Galerkin MFE method, where the time direction is discretized by the BDF2-θ with the WSGD operator, the space direction is approximated by the H^1-Galerkin MFE method, and the fast TT-M algorithm is used to reduce calculation time. The main works and contributions of this article are as follows:

(I) Propose a fast TT-M mixed element method with the WSGD operator to numerically solve the nonlinear pseudo-hyperbolic wave equation with two term fractional derivatives.

(II) Introduce a special auxiliary function, transform the original high-order equation into the coupled system of equations with lower order space-time derivatives, and directly formulate a second-order fully

discrete BDF2-θ H^1-Galerkin MFE system, which can avoid difficulties in numerical calculations and theoretical analysis by directly discretizing fractional derivatives. Further, develop the fast fully discrete TT-M MFE system, and derive optimal a priori error estimates for two functions.
(III) Provide the detailed numerical algorithm by taking smooth and weakly regular solutions. Validate the correctness of the theoretical results and the effectiveness of the numerical algorithm, and illustrate that the TT-M MFE method has good computational efficiency by comparing the calculation results with the standard nonlinear MFE method.

The rest of the article is outlined as follows: In Section 2, the fully discrete scheme based on the combination of an MFE method and the BDF2-θ with the WSGD formula is derived. In Section 3, the optimal error estimates in both L^2-norm and H^1-norm for the fully discrete TT-M MFE scheme are derived. In Section 4, the numerical algorithm is shown. Some experiments in Section 5 are conducted to further confirm our theoretical results. Finally, in Section 6, conclusions and advancements are provided.

2. Weak form and TT-M MFE scheme

Letting $q = {}_0^R D_t^\alpha u_x(x,t) + u_x(x,t)$, we rewrite equation (1.1) as

$$\begin{cases} {}_0^R D_t^\alpha u_x(x,t) + u_x(x,t) = q(x,t), \\ {}_0^R D_t^\beta u(x,t) + u_t - q_x(x,t) + g(u) = f(x,t). \end{cases} \tag{2.1}$$

We multiply the first equation of (2.1) by v_x and the second equation of (2.1) by $-\omega_x$, respectively, then make the inner product on the spatial domain $\bar{\Omega} = [a,b]$ to have

$$\begin{cases} ({}_0^R D_t^\alpha u_x, v_x) + (u_x, v_x) = (q, v_x), \ v \in H_0^1, \\ ({}_0^R D_t^\beta u + u_t, -\omega_x) + (q_x, \omega_x) + (g(u), -\omega_x) = (f, -\omega_x), \ \omega \in H^1. \end{cases} \tag{2.2}$$

For the second equation of (2.2), by the integration by part and the boundary condition

$${}_0^R D_t^\beta u(a,t) = {}_0^R D_t^\beta u(b,t) = 0, 1 \le \beta < 2,$$

we obtain

$$({}_0^R D_t^\beta u + u_t, -\omega_x) = ({}_0^R D_t^{1+\alpha} u_x + u_{tx}, \omega) = (({}_0^R D_t^\alpha u_x + u_x)_t, \omega) = (q_t, \omega).$$

Now, we can get the following mixed weak form

$$\begin{cases} ({}_0^R D_t^\alpha u_x, v_x) + (u_x, v_x) = (q, v_x), \ v \in H_0^1, \\ (q_t, \omega) + (q_x, \omega_x) + (g, -\omega_x) = (f, -\omega_x), \ \omega \in H^1. \end{cases} \tag{2.3}$$

For obtaining the fully discrete TT-M MFE scheme, we introduce the nodes $t_n = n\tau_c (n = 0, 1, 2, \cdots, N)$ in the time interval $[0,T]$, where t_n satisfies $0 = t_0 < t_1 < t_2 < \cdots < t_N = T$ with fine mesh length $\tau = T/NM$ and coarse mesh length $\tau_c = M\tau$ for some positive integer N. Define $u^n = u(\cdot, t_n), q^n = q(\cdot, t_n)$ for smooth functions u and q on $[0,T]$. Some useful lemmas will also be introduced as follows.

Lemma 2.1. ([35]) *With $v(t) \in C^3[0,T]$, at time $t_{n-\theta}$, the following formula with second-order accuracy for approximating the first-order derivative holds*

$$v_t(t_{n-\theta}) = \begin{cases} \partial_t[v^{n-\theta}] + O(\tau^2), \ n \geq 2, \\ \partial_t[v^1] + O(\tau), \ n = 1, \end{cases} \tag{2.4}$$

where

$$\begin{aligned} &\partial_t[v^{n-\theta}] \doteq \frac{(3-2\theta)v^n - (4-4\theta)v^{n-1} + (1-2\theta)v^{n-2}}{2\tau}, \\ &\partial_t[v^1] \doteq \frac{v^1 - v^0}{\tau}, \end{aligned} \tag{2.5}$$

for any $\theta \in [0, \frac{1}{2}]$.

Lemma 2.2. *At time $t_{n-\theta}$, the following important results hold for any $\theta \in [0,1]$ and $v(t) \in C^2[0,T]$,*

$$\begin{aligned} &v(t_{n-\theta}) = (1-\theta)v^n + \theta v^{n-1} + O(\tau^2) \doteq v^{n-\theta} + O(\tau^2), \\ &(1-\theta)g(v^n) + \theta g(v^{n-1}) \doteq g[v^{n-\theta}]. \end{aligned} \tag{2.6}$$

Lemma 2.3. ([29, 35]) *At time t_n, the second-order approximate formula for the Riemann-Liouville fractional derivative with parameter $\gamma \in (0,1)$ holds*

$${}_0^R D_t^\gamma u(t_n) = \tau^{-\gamma} \sum_{i=0}^{n} \mathcal{A}_\gamma(i) v^{n-i} + O(\tau^2) \doteq I_\gamma^n[v^n] + O(\tau^2), \tag{2.7}$$

with

$$\mathcal{A}_\gamma(i) = \begin{cases} \dfrac{\gamma+2}{2} w_0^\gamma, & i = 0, \\ \dfrac{\gamma+2}{2} w_i^\gamma + \dfrac{-\gamma}{2} w_{i-1}^\gamma, & i > 0, \end{cases} \tag{2.8}$$

where series w_i^γ are defined as $w_0^\gamma = 1$, $w_l^\gamma = (-1)^l \binom{\gamma}{l} = \frac{\Gamma(l-\gamma)}{\Gamma(-\gamma)\Gamma(l+1)}, l \geq 1$, which satisfy $w_l^\gamma < 0, w_l^\gamma = (1 - \frac{\gamma+1}{l}) w_{l-1}^\gamma, (l = 1, 2, \cdots), \sum\limits_{l=1}^{\infty} w_l^\gamma = -1$.

Based on the weak form (2.3) and the numerical approximate formulas above, we can get the following equivalent weak form

Case $n = 1$:

$$\begin{aligned} &(I_\alpha^{1-\theta}[u_x^{1-\theta}], v_x) + (u_x^{1-\theta}, v_x) = (q^{1-\theta}, v_x) + (E_1^{1-\theta}, v_x), \\ &(\frac{q^1 - q^0}{\tau}, \omega) + (q_x^{1-\theta}, \omega_x) + (g[u^{1-\theta}], -\omega_x) = (f^{1-\theta}, -\omega_x) + (\sum_{k=1}^{3} \bar{E}_k^{1-\theta}, \omega_x), \end{aligned} \tag{2.9}$$

Case $n \geq 2$:

$$\begin{aligned} &(I_\alpha^{n-\theta}[u_x^{n-\theta}], v_x) + (u_x^{n-\theta}, v_x) = (q^{n-\theta}, v_x) + (E_1^{n-\theta}, v_x), \\ &(\partial_t[q^{n-\theta}], \omega) + (q_x^{n-\theta}, \omega_x) + (g[u^{n-\theta}], -\omega_x) = (f^{n-\theta}, -\omega_x) + (\sum_{k=1}^{3} \bar{E}_k^{n-\theta}, \omega_x), \end{aligned} \tag{2.10}$$

where

$$\begin{aligned}
&\bar{E}_1^{1-\theta} = \partial_t[q^1] - q_t(t_{1-\theta}) = O(\tau),\\
&E_1^{n-\theta} = {}_0^R D_\tau^\alpha u_x^{n-\theta} - I_\alpha^{n-\theta}[u_x^{n-\theta}] = O(\tau^2),\\
&\bar{E}_1^{n-\theta} = \partial_t^{n-\theta}[q] - q_t(t_{n-\theta}) = O(\tau^2),\\
&\bar{E}_2^{n-\theta} = g[u^{n-\theta}] - g(u(t_{n-\theta})) = O(\tau^2),\\
&\bar{E}_3^{n-\theta} = f^{n-\theta} - f(t_{n-\theta}) = O(\tau^2),\\
&I_\alpha^{n-\theta}[u_x^{n-\theta}] \doteq (1-\theta)I_\alpha^n[u_x^n] + \theta I_\alpha^{n-1}[u_x^{n-1}].
\end{aligned} \tag{2.11}$$

We now formulate the fully discrete TT-M MFE system at time $t_{n-\theta}$ for handling the computational time-consuming problems of implicit finite element systems, and we denote U_c^n, Q_c^n as solutions of the system on the time coarse mesh and U_f^m, Q_f^m as solutions of the system on the time fine mesh. The TT-M MFE algorithm can be implemented as the following three steps.

STEP1: First, we arrive at the following nonlinear coupled system based on the time coarse mesh τ_c: Find $(U_c^n, Q_c^n) : [0,T]\times[0,T] \mapsto V_h \times W_h$ such that

Case $n = 1$:

$$\begin{aligned}
&(I_\alpha^{1-\theta}[U_{cx}^{1-\theta}], v_{hx}) + (U_{cx}^{1-\theta}, v_{hx}) = (Q_c^{1-\theta}, v_{hx}),\\
&(\frac{Q_c^1 - Q_c^0}{\tau_c}, \omega_h) + (Q_{cx}^{1-\theta}, \omega_{hx}) + (g[U_c^{1-\theta}], -\omega_{hx}) = (f^{1-\theta}, -\omega_{hx}),
\end{aligned} \tag{2.12}$$

Case $n \geq 2$:

$$\begin{aligned}
&(I_\alpha^{n-\theta}[U_{cx}^{n-\theta}], v_{hx}) + (U_{cx}^{n-\theta}, v_{hx}) = (Q_c^{n-\theta}, v_{hx}),\\
&(\partial_t[Q_c^{n-\theta}], \omega_h) + (Q_{cx}^{n-\theta}, \omega_{hx}) + (g[U_c^{n-\theta}], -\omega_{hx}) = (f^{n-\theta}, -\omega_{hx}).
\end{aligned} \tag{2.13}$$

STEP2: Second, we can get all the interpolated values $U_I^m (m = 0, 1, \cdots, M, M+1, \cdots, 2M, \cdots, NM)$ by using an interpolation formula

$$U_I^m = \lambda_m U_c^{n-1} + (1-\lambda_m)U_c^n, \tag{2.14}$$

where $\lambda_m = n - \frac{m}{M} \in [0,1) (n = \lceil \frac{m}{M} \rceil)$ and $U_I^0 = U_c^0$. Values of Q_I^m can be obtained similarly.

STEP3: Finally, we establish the following linear system on the time fine mesh τ based on the solutions U_I^m, Q_I^m; that is, to find $(U_f^m, Q_f^m) : [0,T]\times[0,T] \mapsto V_h \times W_h$ for any $(v,\omega) \in V_h \times W_h$ such that

Case $m = 1$:

$$\begin{aligned}
&(I_\alpha^{1-\theta}[U_{fx}^{1-\theta}], v_{hx}) + (U_{fx}^{1-\theta}, v_{hx}) = (Q_f^{1-\theta}, v_{hx}),\\
&(\frac{Q_f^1 - Q_f^0}{\tau}, \omega_h) + (Q_{fx}^{1-\theta}, \omega_{hx})\\
&+ (g[U_I^{1-\theta}] + g'[U_I^{1-\theta}](U_f^{1-\theta} - U_I^{1-\theta}), -\omega_{hx}) = (f^{1-\theta}, -\omega_{hx}),
\end{aligned} \tag{2.15}$$

Case $m \geq 2$:

$$\begin{aligned}
&(I_\alpha^{m-\theta}[U_{fx}^{m-\theta}], v_{hx}) + (U_{fx}^{m-\theta}, v_{hx}) = (Q_f^{m-\theta}, v_{hx}),\\
&(\partial_t[Q_f^{m-\theta}], \omega_h) + (Q_{fx}^{m-\theta}, \omega_{hx})\\
&+ (g[U_I^{m-\theta}] + g'[U_I^{m-\theta}](U_f^{m-\theta} - U_I^{m-\theta}), -\omega_{hx}) = (f^{m-\theta}, -\omega_{hx}),
\end{aligned} \tag{2.16}$$

where finite element spaces are defined as

$$V_h = \{v_h | v_h \in \mathbb{P}^k, v_h(a) = v_h(b) = 0, v_{hx} \in L^2, k \in \mathbb{Z}^+\} \subset H_0^1,$$
$$W_h = \{\sigma_h | \sigma_h \in \mathbb{P}^r, \sigma_{hx} \in L^2, r \in \mathbb{Z}^+\} \subset H^1.$$

Remark 2.4. *Here, we provide two other equivalent linearized techniques besides the one mentioned in* (2.15)-(2.16).

$$\begin{aligned} &(a)\ g(U_f^{m-\theta}) \simeq (1-\theta)(g(U_I^m) + g'(U_I^m)(U_f^m - U_I^m)) + \theta g(U_f^{m-1}), \\ &(b)\ g(U_f^{m-\theta}) \simeq g[U_I^{m-\theta}] + (1-\theta)g'(U_I^m)(U_f^m - U_I^m) + \theta g'(U_I^{m-1})(U_f^{m-1} - U_I^{m-1}). \end{aligned} \tag{2.17}$$

3. Error estimates

For subsequent analysis, we introduce some useful lemmas.

Lemma 3.1. ([30, 35]) *Let $\mathcal{A}_\gamma(i)$ be defined in* (2.8)*, then for any positive integer L and real vector $(v^0, v^1, \cdots, v^L) \in R^{L+1}$, the following inequality holds*

$$\sum_{n=0}^{L}\sum_{i=0}^{n} \mathcal{A}_\gamma(i)(v^{n-i}, v^n) \geq 0. \tag{3.1}$$

Lemma 3.2. ([23, 35]) *For series χ^n $(n \geq 2)$, the following inequality holds*

$$\begin{aligned} &(\partial_t[v^{n-\theta}], v^{n-\theta}) \geq \frac{1}{4\tau}(\mathbb{H}[v^n] - \mathbb{H}[v^{n-1}]), \\ &\mathbb{H}[v^n] = (3-2\theta)\|v^n\|^2 - (1-2\theta)\|v^{n-1}\|^2 + (2-\theta)(1-2\theta)\|v^n - v^{n-1}\|^2, \end{aligned} \tag{3.2}$$

and

$$\mathbb{H}[v^n] \geq \frac{1}{1-\theta}\|v^n\|^2, \quad \theta \in [0, \frac{1}{2}]. \tag{3.3}$$

Lemma 3.3. ([47, 48]) *For any function $v \in H_0^1(\Omega)$, we have*

$$\|v\|_{L^4} \leq \|v\|^{\frac{1}{2}}\|v_x\|^{\frac{1}{2}}. \tag{3.4}$$

For considering a priori error estimates for the TT-M MFE system, the projection operator and the inequality should be introduced.

Lemma 3.4. ([36]) *Define an elliptic-projection operator $\Upsilon_h : H_0^1(\Omega) \to V_h$, for any $\phi_h \in V_h$ such that*

$$(u_x - \Upsilon_h u_x, \phi_{hx}) = 0 \tag{3.5}$$

with an estimate inequality

$$\|u - \Upsilon_h u\| + h\|u - \Upsilon_h u\|_1 \leq Ch^{k+1}\|u\|_{k+1}, \ \ \forall u \in H_0^1(\Omega) \cap H^{k+1}(\Omega). \tag{3.6}$$

Lemma 3.5. ([36]) *Define a Ritz-projection operator $\Pi_h : H^1(\Omega) \to W_h$ by*

$$\mathcal{A}(q - \Pi_h q, \chi_h) = 0, \ \forall \chi_h \in W_h, \tag{3.7}$$

where $\mathcal{A}(q, \phi) \doteq (q_x, \phi_x) + \lambda(q, \phi)$, $\mathcal{A}(\phi, \phi) \geq \mu_0\|\phi\|_1^2, \mu_0 > 0$ is a constant. Further, the following estimate inequality holds

$$\|q_t - \Pi_h q_t\| + h\|q - \Pi_h q\|_1 \leq Ch^{r+1}(\|q\|_{r+1} + \|q_t\|_{r+1}), \ \forall q \in H^{r+1}(\Omega). \tag{3.8}$$

Theorem 3.6. *Let $u(\cdot,t_n)$, $q(\cdot,t_n)$ be the solutions of system* (1.1) *and suppose U_c^n, Q_c^n and U_f^m, Q_f^m are the solutions of TT-M MFE systems* (2.12)-(2.13) *and* (2.15)-(2.16)*, respectively, then there exists a constant $C>0$ that depends only on $u(\cdot,t_n)$, $q(\cdot,t_n)$, such that*

$$\begin{aligned}
&\|q^n-Q_c^n\|+\Big(\tau_c\sum_{l=1}^{n}\|u^{l-\theta}-U_c^{l-\theta}\|^2\Big)^{\frac{1}{2}}\le C(\tau_c^2+h^{\min\{k+1,r+1\}}),\\
&\Big(\tau_c\sum_{l=1}^{n}\|u^{l-\theta}-U_c^{l-\theta}\|_1^2\Big)^{\frac{1}{2}}\le C(\tau_c^2+h^{\min\{k,r+1\}}),\\
&\Big(\tau_c\sum_{l=1}^{n}\|q^{l-\theta}-Q_c^{l-\theta}\|_1^2\Big)^{\frac{1}{2}}\le C(\tau_c^2+h^{\min\{k+1,r\}}),
\end{aligned}\tag{3.9}$$

and

$$\begin{aligned}
&\|q^m-Q_f^m\|+\Big(\tau\sum_{l=1}^{m}\|u^{l-\theta}-U_f^{l-\theta}\|^2\Big)^{\frac{1}{2}}\le C(\tau^2+\tau_c^4+h^{\min\{k+1,r+1\}}),\\
&\Big(\tau\sum_{l=1}^{m}\|u^{l-\theta}-U_f^{l-\theta}\|_1^2\Big)^{\frac{1}{2}}\le C(\tau^2+\tau_c^4+h^{\min\{k,r+1\}}),\\
&\Big(\tau\sum_{l=1}^{m}\|q^{l-\theta}-Q_f^{l-\theta}\|_1^2\Big)^{\frac{1}{2}}\le C(\tau^2+\tau_c^4+h^{\min\{k+1,r\}}).
\end{aligned}\tag{3.10}$$

Proof. For convenience, we write error as

$$\begin{aligned}
u^n-U_c^n&=u^n-\Upsilon_h u^n+\Upsilon_h u^n-U_c^n=\eta_c^n+\xi_c^n,\\
q^n-Q_c^n&=q^n-\Pi_h q^n+\Pi_h q^n-Q_c^n=\rho_c^n+\sigma_c^n,\\
u^m-U_f^m&=u^m-\Upsilon_h u^m+\Upsilon_h u^m-U_f^m=\eta_f^m+\xi_f^m,\\
q^m-Q_f^m&=q^m-\Pi_h q^m+\Pi_h q^m-Q_f^m=\rho_f^m+\sigma_f^m.
\end{aligned}$$

(1) Error estimate on the time coarse mesh.

Applying the projection operators in Lemmas 3.4 and 3.5, the error equation on the time coarse mesh is as follows:

Case $n=1$:

$$\begin{aligned}
&(I_\alpha^{1-\theta}[\xi_{cx}^{1-\theta}],v_{hx})+(\xi_{cx}^{1-\theta},v_{hx})=(\rho_c^{1-\theta}+\sigma_c^{1-\theta},v_{hx})+(E_1^{1-\theta},v_x),\\
&(\frac{\sigma_c^1-\sigma_c^0}{\tau_c},\omega_h)+(\sigma_{cx}^{1-\theta},\omega_{hx})+(g[u^{1-\theta}]-g[U_c^{1-\theta}],-\omega_{hx})\\
&=-(\frac{\rho_c^1-\rho_c^0}{\tau_c},\omega_h)+\lambda(\rho_c^{1-\theta},\omega_h)+(\sum_{k=1}^{3}\bar{E}_k^{1-\theta},\omega_{hx}).
\end{aligned}\tag{3.11}$$

Case $n\ge 2$:

$$\begin{aligned}
&(I_\alpha^{n-\theta}[\xi_{cx}^{n-\theta}],v_{hx})+(\xi_{cx}^{n-\theta},v_{hx})=(\rho_c^{n-\theta}+\sigma_c^{n-\theta},v_{hx})+(E_1^{n-\theta},v_{hx}),\\
&(\partial_t[\sigma_c^{n-\theta}],\omega_h)+(\sigma_{cx}^{n-\theta},\omega_{hx})+(g[u^{n-\theta}]-g[U_c^{n-\theta}],-\omega_{hx})\\
&=-(\partial_t[\rho_c^{n-\theta}],\omega_h)+\lambda(\rho_c^{n-\theta},\omega_h)+(\sum_{k=1}^{3}\bar{E}_k^{n-\theta},\omega_{hx}).
\end{aligned}\tag{3.12}$$

Set $\omega_h = \sigma_c^{n-\theta}$ in (3.12), and use Lemma 3.3, the Cauchy-Schwarz inequality, and the Young inequality to obtain

$$\begin{aligned}
&\frac{1}{4\tau_c}(\mathbb{H}(\sigma_c^n) - \mathbb{H}(\sigma_c^{n-1})) + (1-3\varepsilon)\|\sigma_{cx}^{n-\theta}\|^2 \\
\leq&\frac{1}{4\varepsilon}(\|g[u^{n-\theta}] - g[U_c^{n-\theta}]\|^2 + \sum_{k=1}^{3}\|\bar{E}_k^{n-\theta}\|^2) \\
&+ \frac{1}{2}\|\partial_t[\rho_c^{n-\theta}]\|^2 + \frac{1+\lambda}{2}\|\sigma_c^{n-\theta}\|^2 + \frac{\lambda}{2}\|\rho_c^{n-\theta}\|^2 \\
\leq&C(\|\eta_c^{n-\theta}\|^2 + \|\xi_c^{n-\theta}\|^2 + \|\sigma_c^{n-\theta}\|^2 + \tau_c^4) + \frac{1}{2}\|\partial_t[\rho_c^{n-\theta}]\|^2 + \frac{\lambda}{2}\|\rho_c^{n-\theta}\|^2.
\end{aligned} \tag{3.13}$$

Multiply (3.13) by $4\tau_c$, replace n with l, and sum for l from 2 to n to arrive at

$$\begin{aligned}
&\mathbb{H}(\sigma_c^n) + 4\tau_c(1-3\varepsilon)\sum_{l=2}^{n}\|\sigma_{cx}^{l-\theta}\|^2 \\
\leq&\mathbb{H}(\sigma_c^1) + C\tau_c\sum_{l=2}^{n}(\|\eta_c^{l-\theta}\|^2 + \|\xi_c^{l-\theta}\|^2 + \|\sigma_c^{l-\theta}\|^2 + \tau_c^4) \\
&+ 2\tau_c\sum_{l=2}^{n}\|\partial_t[\rho_c^{n-\theta}]\|^2 + 2\tau_c\lambda\sum_{l=2}^{n}\|\rho_c^{l-\theta}\|^2 \\
\leq&\mathbb{H}(\sigma_c^{1-\theta}) + C\tau_c\sum_{l=2}^{n}(\|\xi_c^{l-\theta}\|^2 + \|\sigma_c^{l-\theta}\|^2) + C(h^{2k+2} + h^{2r+2} + \tau_c^4).
\end{aligned} \tag{3.14}$$

Setting $v_h = \xi_c^{n-\theta}$ in (3.12), summing the resulting equation from 1 to n, and using the Cauchy-Schwarz inequality as well as the Young inequality, we have

$$\begin{aligned}
&\sum_{l=1}^{n}(I_\alpha^{l-\theta}[\xi_{cx}^{l-\theta}], \xi_{cx}^{l-\theta}) + \sum_{l=1}^{n}(1-3\varepsilon)\|\xi_{cx}^{l-\theta}\|^2 \\
=&((1-\theta)\tau_c^{-\alpha}\sum_{l=1}^{n}\sum_{i=0}^{l}\mathcal{A}_\alpha(i)\xi_{cx}^{l-i} + \theta\tau_c^{-\alpha}\sum_{l=1}^{n}\sum_{i=0}^{l}\mathcal{A}_\alpha(i)\xi_{cx}^{l-1-i}, \xi_{cx}^{l-\theta}) + \sum_{l=1}^{n}(1-3\varepsilon)\|\xi_{cx}^{l-\theta}\|^2 \\
\leq&\sum_{l=1}^{n}C(\|\rho_c^{l-\theta}\|^2 + \|\sigma_c^{l-\theta}\|^2) + \sum_{l=1}^{n}\|E_1^{l-\theta}\|^2.
\end{aligned} \tag{3.15}$$

Applying Lemma 3.1 and the Poincaré inequality, we obtain, for $n \geq 1$,

$$\begin{aligned}
\tau_c\sum_{l=1}^{n}(1-3\varepsilon)\|\xi_c^{l-\theta}\|^2 \leq&\tau_c\sum_{l=1}^{n}(1-3\varepsilon)\|\xi_{cx}^{l-\theta}\|^2 \\
\leq&C(h^{2r+2} + \tau_c^4) + \tau_c\sum_{l=1}^{n}\|\sigma_c^{l-\theta}\|^2.
\end{aligned} \tag{3.16}$$

For the term $\mathbb{H}(\sigma_c^1)$, we take $\omega_h = \sigma_c^{1-\theta}$ in (3.11) and apply the Cauchy-Schwarz inequality as well as

the Young inequality to have

$$\begin{aligned}
&\|\sigma_c^1\|^2 - \|\sigma_c^0\|^2 + (1-2\theta)\|\sigma_c^1 - \sigma_c^0\|^2 + 2\tau_c\|\sigma_{cx}^{1-\theta}\|^2 \\
\leq& 2\tau_c\|g[u^{1-\theta}] - g[U_c^{1-\theta}]\|\|\sigma_{cx}^{1-\theta}\| + C\sum_{k=1}^{3}\|\tau_c\bar{E}_k^{1-\theta}\|^2 \\
&+ 2\tau_c\varepsilon\|\sigma_{cx}^{1-\theta}\|^2 + 2\varepsilon(1+\tau_c)\|\sigma_c^{1-\theta}\|^2 + C(\|\rho_c^1 - \rho_c^0\|^2 + \|\rho_c^{1-\theta}\|^2) \\
\leq& C(h^{2k+2} + h^{2r+2} + \tau_c^4) + 6\tau_c\varepsilon\|\sigma_{cx}^{1-\theta}\|^2 \\
&+ 2\varepsilon(1+\tau_c)\|\sigma_c^{1-\theta}\|^2 + C\tau_c(\|\xi_c^0\|^2 + \|\xi_c^1\|^2).
\end{aligned} \tag{3.17}$$

Omitting the nonnegative term on the left hand side of (3.17), we obtain

$$\begin{aligned}
&\mathbb{H}(\sigma_c^1) + 2\tau_c(1-3\varepsilon)\|\sigma_{cx}^{1-\theta}\|^2 \\
\leq& C\|\sigma_c^0\|^2 + C(h^{2k+2} + h^{2r+2} + \tau_c^4) + 2\varepsilon(1+\tau_c)\|\sigma_c^{1-\theta}\|^2 + C\tau_c(\|\xi_c^0\|^2 + \|\xi_c^1\|^2).
\end{aligned} \tag{3.18}$$

Substitute (3.18) into (3.14), apply (3.16), and use the Gronwall inequality to have

$$\|\sigma_c^n\|^2 + 2\tau_c(1-3\varepsilon)\sum_{l=1}^{n}\|\sigma_{cx}^{l-\theta}\|^2 \leq C\|\sigma_c^0\|^2 + C(h^{2k+2} + h^{2r+2} + \tau_c^4). \tag{3.19}$$

Notice that the inequalities (3.6) and (3.8) hold; combine (3.16) and (3.19) with the triangle inequality to finish the proof of the first result of Theorem 3.6.

(2) Error estimate on the time fine mesh.

Based on Lemmas 3.4 and 3.5, the error equation on the time fine mesh is as follows:

Case $m = 1$:

$$\begin{aligned}
&(I_\alpha^{1-\theta}[\xi_{fx}^{1-\theta}], v_{hx}) + (\xi_{fx}^{1-\theta}, v_{hx}) = (\rho_f^{1-\theta} + \sigma_f^{1-\theta}, v_{hx}) + (E_1^{1-\theta}, v_{hx}), \\
&(g[u^{1-\theta}] - (g[U_I^{1-\theta}] + g'[U_I^{1-\theta}](U_f^{1-\theta} - U_I^{1-\theta})), -\omega_{hx}) \\
&+ (\frac{\sigma_f^1 - \sigma_f^0}{\tau}, \omega_h) + (\sigma_{fx}^{1-\theta}, \omega_{hx}) \\
=& -(\frac{\rho_f^1 - \rho_f^0}{\tau}, \omega_h) + \lambda(\rho_f^{1-\theta}, \omega_h) + (\sum_{k=1}^{3}\bar{E}_k^{1-\theta}, \omega_{hx}),
\end{aligned} \tag{3.20}$$

Case $m \geq 2$:

$$\begin{aligned}
&(I_\alpha^{m-\theta}[\xi_{fx}^{m-\theta}], v_{hx}) + (\xi_{fx}^{m-\theta}, v_{hx}) = (\rho_f^{m-\theta} + \sigma_f^{m-\theta}, v_{hx}) + (E_1^{m-\theta}, v_{hx}), \\
&(g[u^{m-\theta}] - (g[U_I^{m-\theta}] + g'[U_I^{m-\theta}](U_f^{m-\theta} - U_I^{m-\theta})), -\omega_{hx}) \\
&+ (\partial_t[\sigma_f^{m-\theta}], \omega_h) + (\sigma_{fx}^{m-\theta}, \omega_{hx}) \\
=& -(\partial_t[\rho_f^{m-\theta}], \omega_h) + \lambda(\rho_f^{m-\theta}, \omega_h) + (\sum_{k=1}^{3}\bar{E}_k^{m-\theta}, \omega_{hx}).
\end{aligned} \tag{3.21}$$

For the nonlinear term on the right hand side of (3.21), we use Taylor's formula to get

$$\begin{aligned}
&g[u^{m-\theta}] - (g[U_I^{m-\theta}] + g'[U_I^{m-\theta}](U_f^{m-\theta} - U_I^{m-\theta})) \\
=& g(u^{m-\theta}) + O(\tau^2) - (g(U_I^{m-\theta}) + O(\tau^2) + (g'(U_I^{m-\theta}) + O(\tau^2))(U_f^{m-\theta} - U_I^{m-\theta})) \\
=& g'(U_I^{m-\theta})(\eta_f^{m-\theta} + \xi_f^{m-\theta}) + g''(\bar{U}_I^{m-\theta})(u^{m-\theta} - U_I^{m-\theta})^2 + O(\tau^2).
\end{aligned} \tag{3.22}$$

Set $\omega_h = \sigma_f^{m-\theta}$ in (3.21) and use (3.22), the Cauchy-Schwarz inequality, and the Young inequality to arrive at

$$\begin{aligned}
&\frac{1}{4\tau}(\mathbb{H}(\sigma_f^m) - \mathbb{H}(\sigma_f^{m-1})) + (1-3\varepsilon)\|\sigma_{fx}^{m-\theta}\|^2 \\
\leq&\frac{1}{4\varepsilon}(\|g'(U_I^{m-\theta})\|_\infty^2(\|\eta_f^{m-\theta}\|^2 + \|\xi_f^{m-\theta}\|^2) + \|g''(\bar{U}_I^{m-\theta})\|_\infty^2\|(u^{m-\theta} - U_I^{m-\theta})^2\|^2 \\
&+ \tau^4 + \|\partial_t[\rho_f^{m-\theta}]\|^2 + \lambda\|\rho_f^{m-\theta}\|^2 + \sum_{k=1}^{3}\|\bar{E}_k^{m-\theta}\|^2) + 2\varepsilon\|\sigma_f^{m-\theta}\|^2.
\end{aligned} \tag{3.23}$$

Using a similar derivation to (3.14), we have

$$\begin{aligned}
&\mathbb{H}(\sigma_f^m) + 4\tau(1-3\varepsilon)\sum_{l=2}^{m}\|\sigma_{fx}^{l-\theta}\|^2 \\
\leq&\mathbb{H}(\sigma_f^1) + C\tau\sum_{l=2}^{m}\|u^{l-\theta} - U_I^{l-\theta}\|_{L^4}^4 + C\tau\sum_{l=1}^{m}(\|\xi_f^{l-\theta}\|^2 + \|\sigma_f^{l-\theta}\|^2) \\
&+ (3-2\theta)\int_{t_0}^{t_n}\|\rho_{ft}\|^2 ds + C(h^{2k+2} + h^{2r+2} + \tau^4) \\
\leq&\mathbb{H}(\sigma_f^1) + C\tau\sum_{l=2}^{m}\|u^{l-\theta} - U_I^{l-\theta}\|_{L^4}^4 \\
&+ C\tau\sum_{l=1}^{m}(\|\xi_f^{l-\theta}\|^2 + \|\sigma_f^{l-\theta}\|^2) + C(h^{2k+2} + h^{2r+2} + \tau^4).
\end{aligned} \tag{3.24}$$

To estimate $\mathbb{H}(\sigma_f^1)$, we set $\omega_h = \sigma_f^{1-\theta}$ in (3.20) and apply Taylor's formula to deal with the nonlinear term to arrive at

$$\begin{aligned}
&\|\sigma_f^1\|^2 + (1-2\theta)\|\sigma_f^1 - \sigma_f^0\|^2 + 2\tau\|\sigma_{fx}^{1-\theta}\|^2 \\
=&\|\sigma_f^0\|^2 + 2(\rho_f^1 - \rho_f^0, \sigma_f^{1-\theta}) + 2(\tau\sum_{k=1}^{3}\bar{E}_k^{1-\theta}, \sigma_{fx}^{1-\theta}) + 2\tau\lambda(\rho_f^{1-\theta}, \sigma_f^{1-\theta}) \\
&+ 2\tau(g'(U_I^{1-\theta})(\eta_f^{1-\theta} + \xi_f^{1-\theta}) + g''(\bar{U}_I^{1-\theta})(u^{1-\theta} - U_I^{1-\theta})^2 + O(\tau^2), \sigma_{fx}^{1-\theta}) \\
\leq&C(h^{2k+2} + h^{2r+2} + \tau^4) + 8\varepsilon\tau\|\sigma_{fx}^{1-\theta}\|^2 \\
&+ C\tau(\|(u^{1-\theta} - U_I^{1-\theta})^2\|^2 + \|\sigma_f^{1-\theta}\|^2 + \|\xi_f^{1-\theta}\|^2).
\end{aligned} \tag{3.25}$$

Combining (3.25) with (3.24), we have

$$\begin{aligned}
&\|\sigma_f^m\|^2 + C\tau(1-3\varepsilon)\sum_{l=1}^{m}\|\sigma_{fx}^{l-\theta}\|^2 \\
\leq&C(h^{2k+2} + h^{2r+2} + \tau^4) + C\tau\sum_{l=1}^{m}\|u^{l-\theta} - U_I^{l-\theta}\|_{L^4}^4 + C\tau\sum_{l=1}^{m}(\|\xi_f^{l-\theta}\|^2 + \|\sigma_f^{l-\theta}\|^2).
\end{aligned} \tag{3.26}$$

Setting $v_h = \xi_f^{m-\theta}$ in (3.12) and using a derivation similar to (3.16), we get

$$C\tau\sum_{l=1}^{m}(1-3\varepsilon)\|\xi_f^{l-\theta}\|^2 \leq C\tau\sum_{l=1}^{m}(1-3\varepsilon)\|\xi_{fx}^{l-\theta}\|^2 \leq C(h^{2r+2} + \tau^4) + \tau\sum_{l=1}^{m}\|\sigma_f^{l-\theta}\|^2. \tag{3.27}$$

We now estimate the error $C\tau \sum_{l=1}^{m} \|u^{l-\theta} - U_I^{l-\theta}\|_{L^4}^4$. Denote $n = \lceil \frac{l}{M} \rceil$ as the smallest integer that is equal to or greater than $\frac{l}{M}$, then by the notations introduced in (2.14), we get

$$\begin{aligned} u^l &= \lambda_l u^{n-1} + (1-\lambda_l)u^n + C\tau_c^2 u_{tt}(\bar{t}_l), \\ U_I^l &= \lambda_l U_c^{n-1} + (1-\lambda_l)U_c^n, \end{aligned} \tag{3.28}$$

where $\bar{t}_{l-\theta} \in (t_{n-\theta-1}, t_{n-\theta})$. For $\lambda_l \in [0, \frac{1}{2}]$, follow the idea from [46] and use (3.9) and (3.28) to obtain the following result

$$\begin{aligned} & C\tau \sum_{l=1}^{m} \|u^{l-\theta} - U_I^{l-\theta}\|^2 \\ \leq & C\tau \sum_{l=1}^{m} (\|(1-\theta)(u^{n-\lambda_l} - U_c^{n-\lambda_l}) + \theta(u^{n-1-\lambda_l} - U_c^{n-1-\lambda_l})\|^2 + \tau_c^4) \\ \leq & C\tau \sum_{l=1}^{m} (\|u^{n-\lambda_l} - U_c^{n-\lambda_l}\|^2 + \|u^{n-1-\lambda_l} - U_c^{n-1-\lambda_l}\|^2 + \tau_c^4) \\ \leq & C\tau \sum_{k=0}^{\lceil \frac{m}{M} \rceil - 1} \sum_{l=1+kM}^{M+kM} (\|u^{k+1-\lambda_l} - U_c^{k+1-\lambda_l}\|^2 + \|u^{k-\lambda_l} - U_c^{k-\lambda_l}\|^2 + \tau_c^4) \\ \leq & C\tau_c \sum_{k=0}^{n} (\|u^{k-\lambda_l} - U_c^{k-\lambda_l}\|^2 + \tau_c^4) \\ \leq & C(\tau_c^4 + h^{\min\{2k+2,\, 2r+2\}}). \end{aligned} \tag{3.29}$$

Using the techniques applied to (3.29), we easily get the inequality

$$\begin{aligned} C\tau \sum_{l=1}^{m} \|(u^{l-\theta} - U_I^{l-\theta})_x\|^2 \leq & C\tau_c \sum_{k=0}^{n} \|(u^{k-\theta} - U_c^{k-\theta})_x\|^2 \\ \leq & C(\tau_c^4 + h^{\min\{2k,2r+2\}}). \end{aligned} \tag{3.30}$$

Making use of Lemma 3.3, (3.30), and (3.29), we can obtain

$$\begin{aligned} C\tau \sum_{l=1}^{m} \|u^{l-\theta} - U_I^{l-\theta}\|_{L^4}^4 \leq & C\tau \sum_{l=1}^{m} \|u^{l-\theta} - U_I^{l-\theta}\|^2 \|(u^{l-\theta} - U_I^{l-\theta})_x\|^2 \\ \leq & C\tau \sum_{l=1}^{m} (\|u^{l-\theta} - U_I^{l-\theta}\|^4 + \|(u^{l-\theta} - U_I^{l-\theta})_x\|^4) \\ \leq & C(h^{\min\{4r+4,4k\}} + \tau_c^8). \end{aligned} \tag{3.31}$$

Substitute (3.27) and (3.31) into (3.26) and apply the Gronwall inequality to obtain

$$\|\sigma_f^m\|^2 + C\tau(1-4\varepsilon) \sum_{l=1}^{m} \|\sigma_{fx}^{l-\theta}\|^2 \leq C(h^{\min\{2r+2,2k+2\}} + \tau^4 + \tau_c^8). \tag{3.32}$$

Combine (3.27), (3.30), (3.32) and (3.6) with (3.8) and use the triangle inequality to finish the proof of the second result of Theorem 3.6.

4. Numerical algorithm

In this section, we provide a numerical algorithm for solving the examples with smooth solutions and weakly regular solutions. For the solution u with weak regularity, referring to [49, 50], we split it into the smooth part and the weak regular part as the following

$$u = u_1 + u_2 = \sum_{k=1}^{j} c_k t^{\sigma_k} + t^{\sigma_{j+1}} \varrho, \tag{4.1}$$

where $c_k = c_k(x)$ are coefficient functions, parameters σ_k satisfy $0 \le \sigma_1 < \cdots < \sigma_{j+1}$, $\sigma_j < 3$ and $\sigma_{j+1} \ge 3$ and ϱ is sufficiently smooth with respect to t. Thus, we can think of u_1 as the nonsmooth part of the u, which may cause a loss of accuracy in time. For solving this problem, based on the idea presented in [51], we develop a corrected technique by adding correction parts. We now discretize the spatial domain $\bar{\Omega}$ as $a = x_0 < x_1 < \cdots < x_L = b$, where the nodes are $x_k = x_0 + kh$ with the uniform spatial step size $h = \frac{b-a}{L}$. Next, considering mixed linear element spaces with linear basis functions $\{\phi_i(x)\}_{i=0}^{L}$ and $\{\varphi_i(x)\}_{i=0}^{L}$, we can write numerical solution U_c and Q_c as: $U_c^n = \sum\limits_{i=0}^{L} u_i^n \phi_i$, $Q_c^n = \sum\limits_{i=0}^{L} q_i^n \varphi_i$, respectively. Based on the numerical scheme (2.12)-(2.13) combined with the corrected technique, we formulate a numerical algorithm in the matrix form.
Case $n = 1$:

$$\begin{aligned}
&\mathbf{B}_1((1-\theta)\tau_c^{-\alpha}\mathcal{A}_\alpha(0)\mathbf{u}_c^1 + \tau^{-\alpha}\sum_{k=1}^{j}\omega_{1,k}^{(\alpha)}\mathbf{u}_c^k) + \mathbf{B}_1((1-\theta)\mathbf{u}_c^1 + \sum_{k=1}^{j}\omega_{1,k}^{(0)}\mathbf{u}_c^k) = \mathbf{C}((1-\theta)\mathbf{q}_c^1 + \sum_{k=1}^{j+1}\bar{\omega}_{1,k}^{(0)}\mathbf{q}_c^k),\\
&\mathbf{A}(\tau_c^{-1}\mathbf{q}_c^1 + \tau_c^{-1}\sum_{k=1}^{j+1}\tilde{\omega}_{1,k}^{(1)}\mathbf{q}_c^k) + \mathbf{B}_2((1-\theta)\mathbf{q}_c^1 + \sum_{k=1}^{j+1}\bar{\omega}_{1,k}^{(0)}\mathbf{q}_c^k) = -\mathbf{F}^{1-\theta} + (1-\theta)\mathbf{C}g(\mathbf{u}_c^1),
\end{aligned} \tag{4.2}$$

Case $n \ge 2$:

$$\begin{aligned}
&\mathbf{B}_1((1-\theta)\tau_c^{-\alpha}\sum_{i=0}^{n}\mathcal{A}_\alpha(n-i)\mathbf{u}_c^i + \theta\tau_c^{-\alpha}\sum_{i=0}^{n-1}\mathcal{A}_\alpha(n-1-i)\mathbf{u}_c^i + \tau^{-\alpha}\sum_{k=1}^{j}\omega_{n,k}^{(\alpha)}\mathbf{u}_c^k)\\
&+ \mathbf{B}_1((1-\theta)\mathbf{u}_c^n + \theta\mathbf{u}_c^{n-1} + \sum_{k=1}^{j}\omega_{n,k}^{(0)}\mathbf{u}_c^k) = \mathbf{C}((1-\theta)\mathbf{q}_c^n + \theta\mathbf{q}_c^{n-1} + \sum_{k=1}^{j+1}\bar{\omega}_{n,k}^{(0)}\mathbf{q}_c^k),\\
&\mathbf{A}(\tau_c^{-1}\frac{3-2\theta}{2}\mathbf{q}_c^n - \tau_c^{-1}\frac{4-4\theta}{2}\mathbf{q}_c^{n-1} + \tau_c^{-1}\frac{1-2\theta}{2}\mathbf{q}_c^{n-2} + \tau_c^{-1}\sum_{k=1}^{j+1}\bar{\omega}_{n,k}^{(1)}\mathbf{q}_c^k)\\
&+ \mathbf{B}_2((1-\theta)\mathbf{q}_c^n + \theta\mathbf{q}_c^{n-1} + \sum_{k=1}^{j+1}\bar{\omega}_{n,k}^{(0)}\mathbf{q}_c^k) = -\mathbf{F}^{n-\theta} + \mathbf{C}((1-\theta)g(\mathbf{u}_c^n) + \theta g(\mathbf{u}_c^{n-1})),
\end{aligned} \tag{4.3}$$

where

$$\mathbf{A} = [(\varphi_i, \varphi_j)]^T_{0\leqslant i,j\leqslant L} = \frac{1}{L}\begin{pmatrix} \frac{1}{3} & \frac{1}{6} & 0 & \cdots & \cdots & 0 \\ \frac{1}{6} & \frac{2}{3} & \frac{1}{6} & 0 & \cdots & 0 \\ \vdots & \ddots & \ddots & \ddots & \ddots & \vdots \\ 0 & 0 & \cdots & 0 & \frac{1}{6} & \frac{1}{3} \end{pmatrix},$$

$$\mathbf{B}_1 = \Big[(\frac{\phi_i}{\partial x}, \frac{\phi_j}{\partial x})\Big]^T_{0\leqslant i,j\leqslant L} = L\begin{pmatrix} 1 & 0 & 0 & \cdots & \cdots & 0 \\ 0 & 2 & -1 & 0 & \cdots & 0 \\ \vdots & \ddots & \ddots & \ddots & \ddots & \vdots \\ 0 & 0 & \cdots & 0 & 0 & 1 \end{pmatrix},$$

$$\mathbf{B}_2 = \Big[(\frac{\varphi_i}{\partial x}, \frac{\varphi_j}{\partial x})\Big]^T_{0\leqslant i,j\leqslant L} = L\begin{pmatrix} 1 & -1 & 0 & \cdots & \cdots & 0 \\ -1 & 2 & -1 & 0 & \cdots & 0 \\ \vdots & \ddots & \ddots & \ddots & \ddots & \vdots \\ 0 & 0 & \cdots & 0 & -1 & 1 \end{pmatrix}, \tag{4.4}$$

$$\mathbf{C} = \Big[(\varphi_i, \frac{\varphi_j}{\partial x})\Big]^T_{0\leqslant i,j\leqslant L} = \begin{pmatrix} -\frac{1}{2} & \frac{1}{2} & 0 & \cdots & \cdots & 0 \\ -\frac{1}{2} & 0 & \frac{1}{2} & 0 & \cdots & 0 \\ \vdots & \ddots & \ddots & \ddots & \ddots & \vdots \\ 0 & 0 & \cdots & 0 & -\frac{1}{2} & \frac{1}{2} \end{pmatrix},$$

$$\mathbf{u}_c^n = [u_0^n, u_1^n \cdots, u_L^n]^T, \mathbf{q}_c^n = [q_0^n, q_1^n \cdots, q_L^n]^T,$$

$$\mathbf{F} = \Big[\Big(f, \frac{\varphi_0}{\partial x}\Big), \Big(f, \frac{\varphi_1}{\partial x}\Big), \cdots, \Big(f, \frac{\varphi_L}{\partial x}\Big)\Big]^T.$$

In the above algorithm, $\{\omega_{n,k}^{(\alpha)}\}_{k=1}^{j}$, $\{\omega_{n,k}^{(0)}\}_{k=1}^{j}$ are correction weights of $I_\alpha^{n-\theta}[U_{cx}^{n-\theta}]$, $U_{cx}^{n-\theta}$, respectively. $\{\bar{\omega}_{n,k}^{(0)}\}_{k=1}^{j+1}$ are correction weights of $Q_c^{n-\theta}$. $\{\tilde{\omega}_{1,k}^{(1)}\}_{k=1}^{j+1}$ are correction weights of $\partial_t[u^1]$. $\{\bar{\omega}_{n,k}^{(1)}\}_{k=1}^{j+1}$ are correction weights of $\partial_t[u^{n-\theta}]$. The correction weights $\{\omega_{n,k}^{(\alpha)}\}_{k=1}^{j}$ can be obtained by the following formula [51]

$$\sum_{k=1}^{j} \omega_{n,k}^{(\alpha)} k^m = \frac{\Gamma(m+1)}{\Gamma(m-\alpha+1)}(n-\theta)^{m-\alpha} - \sum_{k=1}^{n} \hat{\mathcal{A}}_\alpha(n-k)k^m, m = \sigma_1, \cdots, \sigma_j, \tag{4.5}$$

where

$$\hat{\mathcal{A}}_\alpha(0) = (1-\theta)\mathcal{A}_\alpha(0), \hat{\mathcal{A}}_\alpha(n) = (1-\theta)\mathcal{A}_\alpha(n) + \theta\mathcal{A}_\alpha(n-1)\ (n \geq 2).$$

Similarly, we can get the correction coefficients $\{\omega_{n,k}^{(0)}\}_{k=1}^{j}$, $\{\bar{\omega}_{n,k}^{(0)}\}_{k=1}^{j+1}$, $\{\bar{\omega}_{n,k}^{(1)}\}_{k=1}^{j+1}$, and $\{\tilde{\omega}_{1,k}^{(1)}\}_{k=1}^{j+1}$ by using (4.5).

We divide the calculation process into two parts. First, we calculate $\mathbf{u}_c^k$ and $\mathbf{q}_c^k$ by (4.4)-(4.5), where $k = 1, 2, \cdots, j+1$, then we can obtain $\mathbf{u}_c^m$ and $\mathbf{q}_c^m, m > j+1$ by $\mathbf{u}_c^k$ and $\mathbf{q}_c^k$. The process of computation on the fine mesh is similar to that on the coarse mesh, so we will not introduce details here.

5. Numerical tests

Here, for showing the feasibility and validity of our numerical method and the efficiency of the TT-M MFE system, we consider a linear element and provide the computing results by our numerical procedure.

5.1. Example 1

In this example, we use the linearized method (2.17)(a) to finish our calculations. Considering the space domain $\bar{\Omega} = [0, 1]$ and the time interval $\bar{J} = [0, 1]$, we take the nonlinear term $g(u) = u^3 - u$, the following given source term

$$f(x,t) = (\frac{\Gamma(4+\alpha)}{\Gamma(3)}t^2 + (3+\alpha)t^{2+\alpha} + \frac{\Gamma(4+\alpha)}{\Gamma(4)}t^3\pi^2 + t^{3+\alpha}\pi^2 - t^{3+\alpha})\sin\pi x + (t^{3+\alpha}\sin\pi x)^3,$$

and then easily validate that the exact solution is $u = t^{3+\alpha}\sin\pi x$ and the corresponding auxiliary function is $q = \frac{\Gamma(4+\alpha)}{\Gamma(4)}t^3\pi\cos\pi x + t^{3+\alpha}\pi\cos\pi x$.

Table 1. Spatial convergence results with $\tau = \frac{1}{10000}$ for MFE method (Example 1).

α	θ	h	$\|u - u_h\|$	rate	$\|q - q_h\|$	rate	CPU(s)
		1/200	4.5123E-05	-	6.9060E-04	-	106
	0.1	1/300	2.0078E-05	1.9971	3.0697E-04	1.9997	151
		1/400	1.1299E-05	1.9983	1.7268E-04	1.9998	271
		1/200	4.5124E-05	-	6.9060E-04	-	111
0.3	0.3	1/300	2.0079E-05	1.9971	3.0697E-04	1.9997	155
		1/400	1.1300E-05	1.9982	1.7268E-04	1.9998	285
		1/200	4.5125E-05	-	6.9060E-04	-	112
	0.5	1/300	2.0079E-05	1.9970	3.0697E-04	1.9997	153
		1/400	1.1301E-05	1.9982	1.7268E-04	1.9998	269
		1/200	4.5596E-05	-	1.1129E-03	-	111
	0.1	1/300	2.0282E-05	1.9979	4.9470E-04	1.9997	167
		1/400	1.1409E-05	1.9999	2.7828E-04	1.9998	300
		1/200	4.5597E-05	-	1.1130E-03	-	109
0.8	0.3	1/300	2.0283E-05	1.9978	4.9470E-04	1.9997	156
		1/400	1.1410E-05	1.9997	2.7828E-04	1.9998	285
		1/200	4.5599E-05	-	1.1130E-03	-	107
	0.5	1/300	2.0285E-05	1.9977	4.9470E-04	1.9997	153
		1/400	1.1412E-05	1.9996	2.7829E-04	1.9998	271
		1/200	4.5585E-05	-	1.3908E-03	-	109
	0.1	1/300	2.0273E-05	1.9985	6.1820E-04	1.9997	144
		1/400	1.1400E-05	2.0010	3.4776E-04	1.9998	249
		1/200	4.5587E-05	-	1.3908E-03	-	97
0.99	0.3	1/300	2.0274E-05	1.9984	6.1821E-04	1.9997	141
		1/400	1.1401E-05	2.0010	3.4776E-04	1.9998	251
		1/200	4.5588E-05	-	1.3908E-03	-	118
	0.5	1/300	2.0276E-05	1.9983	6.1821E-04	1.9997	154
		1/400	1.1403E-05	2.0007	3.4776E-04	1.9998	275

Table 2. Spatial convergence results with $\tau = \frac{1}{10000}$ for TT-M MFE method (Example 1).

α	θ	h	$\|u - U_f\|$	rate	$\|q - Q_f\|$	rate	CPU(s)
		1/200	4.5123E-05	-	6.9060E-04	-	70
	0.1	1/300	2.0078E-05	1.9971	3.0697E-04	1.9997	97
		1/400	1.1299E-05	1.9983	1.7268E-04	1.9998	150
		1/200	4.5124E-05	-	6.9060E-04	-	77
0.3	0.3	1/300	2.0079E-05	1.9971	3.0697E-04	1.9997	105
		1/400	1.1300E-05	1.9982	1.7268E-04	1.9998	161
		1/200	4.5125E-05	-	6.9060E-04	-	75
	0.5	1/300	2.0079E-05	1.9970	3.0697E-04	1.9997	102
		1/400	1.1301E-05	1.9982	1.7268E-04	1.9998	159
		1/200	4.5596E-05	-	1.1129E-03	-	72
	0.1	1/300	2.0282E-05	1.9979	4.9470E-04	1.9997	95
		1/400	1.1409E-05	1.9999	2.7828E-04	1.9998	159
		1/200	4.5597E-05	-	1.1130E-03	-	76
0.8	0.3	1/300	2.0283E-05	1.9978	4.9470E-04	1.9997	100
		1/400	1.1410E-05	1.9997	2.7828E-04	1.9998	158
		1/200	4.5599E-05	-	1.1130E-03	-	77
	0.5	1/300	2.0285E-05	1.9977	4.9470E-04	1.9997	102
		1/400	1.1412E-05	1.9996	2.7829E-04	1.9998	168
		1/200	4.5585E-05	-	1.3908E-03	-	77
	0.1	1/300	2.0273E-05	1.9985	6.1820E-04	1.9997	104
		1/400	1.1400E-05	2.0010	3.4776E-04	1.9998	159
		1/200	4.5587E-05	-	1.3908E-03	-	69
0.99	0.3	1/300	2.0274E-05	1.9984	6.1821E-04	1.9997	92
		1/400	1.1402E-05	2.0008	3.4776E-04	1.9998	147
		1/200	4.5588E-05	-	1.3908E-03	-	71
	0.5	1/300	2.0276E-05	1.9983	6.1821E-04	1.9997	94
		1/400	1.1403E-05	2.0006	3.4776E-04	1.9998	144

In Table 1, with the fixed time step length $\tau = \frac{1}{10000}$, changed space step length $h = \frac{1}{200}, \frac{1}{300}, \frac{1}{400}$, fractional parameter $\alpha = 0.3, 0.8, 0.99$, and shifted parameter $\theta = 0.1, 0.3, 0.5$, we calculate the spatial convergence results of the standard nonlinear mixed element algorithm under different parameters and record the Central Processing Unit (CPU) time required for the algorithm. One can see that for the currently selected exact solution, the spatial convergence results are optimal, which is consistent with the theoretical results of the linear element ($k = r = 1$) we selected. Further, in Table 2, based on the chosen changed parameters as in Table 1 with the fixed time step length $\tau = \tau_c/M = 1/NM = 1/10000$ ($N = M = 100$) for the TT-M MFE method, we get the optimal convergence results and CPU time. Comparing the data in Tables 1–2, one can see that the fast TT-M MFE algorithm can greatly reduce the CPU time while maintaining the same convergence accuracy as the standard nonlinear mixed element method.

Table 3. Temporal convergence results with $h = \frac{1}{5000}$ for MFE method (Example 1).

α	θ	τ	$\|u - u_h\|$	rate	$\|q - q_h\|$	rate	CPU(s)
		1/144	1.9638E-05	-	5.7720E-05	-	668
	0.1	1/256	6.1726E-06	2.0115	1.8140E-05	2.0117	1216
		1/400	2.4869E-06	2.0370	7.3284E-06	2.0309	1720
		1/144	1.6339E-05	-	3.7840E-05	-	690
0.3	0.3	1/256	5.1271E-06	2.0144	1.1854E-05	2.0173	1273
		1/400	2.0589E-06	2.0443	4.7657E-06	2.0418	1977
		1/144	1.3111E-05	-	1.7996E-05	-	630
	0.5	1/256	4.0930E-06	2.0234	5.5921E-06	2.0314	1116
		1/400	1.6332E-06	2.0586	2.2216E-06	2.0685	1868
		1/144	7.8075E-05	-	1.1170E-04	-	677
	0.1	1/256	2.4724E-05	1.9986	3.5135E-05	2.0103	1228
		1/400	1.0097E-05	2.0067	1.4196E-05	2.0306	1736
		1/144	7.1921E-05	-	7.4946E-05	-	717
0.8	0.3	1/256	2.2772E-05	1.9988	2.3504E-05	2.0154	1211
		1/400	9.2964E-06	2.0074	9.4544E-06	2.0406	1725
		1/144	6.5762E-05	-	3.8475E-05	-	698
	0.5	1/256	2.0819E-05	1.9990	1.1988E-05	2.0267	1232
		1/400	8.4963E-06	2.0082	4.7745E-06	2.0628	1711
		1/144	1.1956E-04	-	1.4295E-04	-	699
	0.1	1/256	3.7914E-05	1.9961	4.4975E-05	2.0098	1128
		1/400	1.5512E-05	2.0026	1.8174E-05	2.0303	1881
		1/144	1.1208E-04	-	9.6687E-05	-	717
0.99	0.3	1/256	3.5542E-05	1.9962	3.0333E-05	2.0148	1223
		1/400	1.4540E-05	2.0029	1.2204E-05	2.0401	1731
		1/144	1.0459E-04	-	5.0833E-05	-	621
	0.5	1/256	3.3168E-05	1.9961	1.5850E-05	2.0254	1193
		1/400	1.3567E-05	2.0031	6.3173E-06	2.0612	1724

Table 4. Temporal convergence results with $h = \frac{1}{5000}$ for TT-M MFE method (Example 1).

α	θ	τ	$\|u - U_f\|$	rate	$\|q - Q_f\|$	rate	CPU(s)
		1/144	1.9731E-05	-	5.7726E-05	-	500
	0.1	1/256	6.1900E-06	2.0148	1.8141E-05	2.0118	822
		1/400	2.4907E-06	2.0398	7.3285E-06	2.0310	1176
		1/144	1.6388E-05	-	3.7843E-05	-	466
0.3	0.3	1/256	5.1364E-06	2.0165	1.1854E-05	2.0174	827
		1/400	2.0611E-06	2.0460	4.7658E-06	2.0418	1272
		1/144	1.3054E-05	-	1.7998E-05	-	439
	0.5	1/256	4.0850E-06	2.0192	5.5923E-06	2.0315	759
		1/400	1.6312E-06	2.0570	2.2216E-06	2.0686	1190
		1/144	7.8511E-05	-	1.1171E-04	-	441
	0.1	1/256	2.4805E-05	2.0025	3.5137E-05	2.0103	754
		1/400	1.0119E-05	2.0092	1.4196E-05	2.0307	1142
		1/144	7.2194E-05	-	7.4953E-05	-	484
0.8	0.3	1/256	2.2823E-05	2.0015	2.3505E-05	2.0155	833
		1/400	9.3104E-06	2.0091	9.4547E-06	2.0406	1278
		1/144	6.5901E-05	-	3.8479E-05	-	478
	0.5	1/256	2.0845E-05	2.0005	1.1989E-05	2.0268	809
		1/400	8.5034E-06	2.0092	4.7747E-06	2.0629	1278
		1/144	1.2014E-04	-	1.4296E-04	-	475
	0.1	1/256	3.8023E-05	1.9995	4.4978E-05	2.0098	818
		1/400	1.5541E-05	2.0048	1.8175E-05	2.0304	1223
		1/144	1.1245E-04	-	9.6696E-05	-	442
0.99	0.3	1/256	3.5611E-05	1.9985	3.0335E-05	2.0149	767
		1/400	1.4558E-05	2.0044	1.2204E-05	2.0401	1210
		1/144	1.0479E-04	-	5.0837E-05	-	440
	0.5	1/256	3.3206E-05	1.9975	1.5851E-05	2.0255	742
		1/400	1.3576E-05	2.0041	6.3175E-06	2.0613	1240

In Tables 3–4, by taking the space step length $h = 1/5000$, time step length $\tau = 1/144, 1/256, 1/400$ ($\tau = \tau_c^2$ for TT-M method), time fractional parameter α as $0.3, 0.8, 0.99$, and shifted parameter θ as $0.1, 0.3, 0.5$, we implement the numerical calculations by using standard nonlinear MFE method and fast TT-M MFE method, respectively. From this, one can see that these two methods have almost the same error results and time convergence rate, and that our TT-M MFE algorithm can save the CPU time.

5.2. Example 2

In this example, we continue to use the linearization technique (2.17)(a) to verify the efficiency of the current TT-M MFE algorithm. Considering the space-time domain $\bar{\Omega} \times \bar{J} = [0, 1] \times [0, 1]$, we choose the nonlinear term $g(u) = \arctan u$ and the source term $f(x, t) = 100 \sin^2(5\pi t) \sin^2(3\pi x)[0.15 - (t - \frac{1}{2})^2 -$

$(x-\frac{1}{2})^2]^2$. Here, we just consider the TT-M MFE algorithm with $M = 4$. Because of the unknown exact solution, we choose the numerical solution with $h = \tau = \frac{1}{1200}$ as the approximating exact solution.

Table 5. Spatial convergence results with $\tau = \frac{1}{1200}$ for TT-M MFE method (Example 2).

α	θ	h	$\|u - U_f\|$	rate	$\|q - Q_f\|$	rate
		1/30	8.6102E-04	-	2.1992E-02	-
	0.1	1/40	4.7269E-04	2.0845	1.2031E-02	2.0969
		1/50	2.9250E-04	2.1510	7.3662E-03	2.1984
		1/30	8.6103E-04	-	2.1992E-02	-
0.3	0.3	1/40	4.7270E-04	2.0845	1.2031E-02	2.0969
		1/50	2.9250E-04	2.1510	7.3662E-03	2.1984
		1/30	8.6104E-04	-	2.1992E-02	-
	0.5	1/40	4.7270E-04	2.0845	1.2031E-02	2.0969
		1/50	2.9251E-04	2.1510	7.3662E-03	2.1984
		1/30	7.2514E-04	-	2.1991E-02	-
	0.1	1/40	3.9992E-04	2.0686	1.2030E-02	2.0969
		1/50	2.4819E-04	2.1380	7.3660E-03	2.1983
		1/30	7.2515E-04	-	2.1991E-02	-
0.5	0.3	1/40	3.9993E-04	2.0686	1.2030E-02	2.0969
		1/50	2.4819E-04	2.1380	7.3660E-03	2.1983
		1/30	7.2516E-04	-	2.1991E-02	-
	0.5	1/40	3.9993E-04	2.0686	1.2030E-02	2.0969
		1/50	2.4819E-04	2.1380	7.3660E-03	2.1983
		1/30	5.3808E-04	-	2.1989E-02	-
	0.1	1/40	3.0067E-04	2.0231	1.2029E-02	2.0968
		1/50	1.8816E-04	2.1004	7.3656E-03	2.1983
		1/30	5.3809E-04	-	2.1989E-02	-
0.99	0.3	1/40	3.0067E-04	2.0231	1.2029E-02	2.0968
		1/50	1.8816E-04	2.1004	7.3656E-03	2.1983
		1/30	5.3809E-04	-	2.1989E-02	-
	0.5	1/40	3.0067E-04	2.0231	1.2029E-02	2.0968
		1/50	1.8816E-04	2.1004	7.3656E-03	2.1983

In Table 5, with the fixed time step length $\tau = \tau_c/M = 1/NM = 1/1200$, changed space step length $h = 1/30, 1/40, 1/50$, fractional parameter $\alpha = 0.3, 0.5, 0.99$, and shifted parameter $\theta = 0.1, 0.3, 0.5$, we can get the errors and spatial convergence results of the TT-M MFE system. In Table 6, considering the fixed space step length $h = 1/1200$, fine time step length $\tau = \tau_c/M = 1/NM = 1/80, 1/100, 1/120$ ($N = 20, 25, 30$), fractional parameter $\alpha = 0.3, 0.5, 0.99$ and shifted parameter $\theta = 0.1, 0.3, 0.5$, we calculate the error results and time convergence rate for the TT-M MFE algorithm. The computed data shows that the TT-M MFE algorithm can also maintain a good calculation effect for the selected numerical example with an unknown exact solution.

Table 6. Temporal convergence results with $h = \frac{1}{1200}$ for TT-M MFE method (Example 2).

α	θ	τ	$\|u - U_f\|$	rate	$\|q - Q_f\|$	rate
		1/80	3.6618E-03	-	3.9369E-02	-
	0.1	1/100	2.3445E-03	1.9981	2.5898E-02	1.8768
		1/120	1.6378E-03	1.9675	1.8949E-02	1.7138
		1/80	2.6086E-03	-	2.7341E-02	-
0.3	0.3	1/100	1.6788E-03	1.9752	1.7193E-02	2.0789
		1/120	1.1734E-03	1.9643	1.1632E-02	2.1430
		1/80	1.5372E-03	-	1.2016E-02	-
	0.5	1/100	9.8788E-04	1.9815	7.7099E-03	1.9884
		1/120	6.9141E-04	1.9572	5.2103E-03	2.1493
		1/80	2.5340E-03	-	3.9413E-02	-
	0.1	1/100	1.6204E-03	2.0037	2.5947E-02	1.8733
		1/120	1.1305E-03	1.9749	1.8978E-02	1.7157
		1/80	1.9061E-03	-	2.7370E-02	-
0.5	0.3	1/100	1.2434E-03	1.9143	1.7208E-02	2.0798
		1/120	8.7143E-04	1.9498	1.1652E-02	2.1386
		1/80	1.3166E-03	-	1.2030E-02	-
	0.5	1/100	8.5443E-04	1.9378	7.7174E-03	1.9896
		1/120	5.9639E-04	1.9720	5.2145E-03	2.1502
		1/80	1.1108E-03	-	3.9446E-02	-
	0.1	1/100	6.9195E-04	2.1212	2.5989E-02	1.8699
		1/120	4.6577E-04	2.1709	1.9001E-02	1.7178
		1/80	7.8786E-04	-	2.7394E-02	-
0.99	0.3	1/100	5.0252E-04	2.0153	1.7219E-02	2.0807
		1/120	3.4426E-04	2.0746	1.1668E-02	2.1343
		1/80	5.5433E-04	-	1.2043E-02	-
	0.5	1/100	3.6261E-04	1.9020	7.7234E-03	1.9909
		1/120	2.5445E-04	1.9428	5.2176E-03	2.1512

Further, in order to check the behaviors of numerical solution, we provide the comparison figures of numerical solutions between different time step length sizes. In Figure 1, we show the comparison surfaces of numerical solutions U_f with the fixed space step length $h = 1/1200$, fractional parameter $\alpha = 0.3$, shifted parameter $\theta = 0.1$, and changed time step length $\tau = 1/120, 1/1200$. We also provide the comparison surfaces of numerical solutions Q_f in Figure 2. The comparison results tell us the corresponding numerical solutions have similar behavior. Moreover, in Figure 3, for fixed fractional parameter $\alpha = 0.3$ and parameter $\theta = 0.1$, we depict the figures of difference in L^2-norm between reference solution with $h = \tau = 1/1200$ and numerical solution with $h = 1/1200$ and $\tau = 1/120$, from which one can see the performances of $\|u^n - U_f^n\|$ and $\|q^n - Q_f^n\|$. It is easy to see the changes of actual errors at different time nodes from the figures, which can reveal the overall distribution of errors.

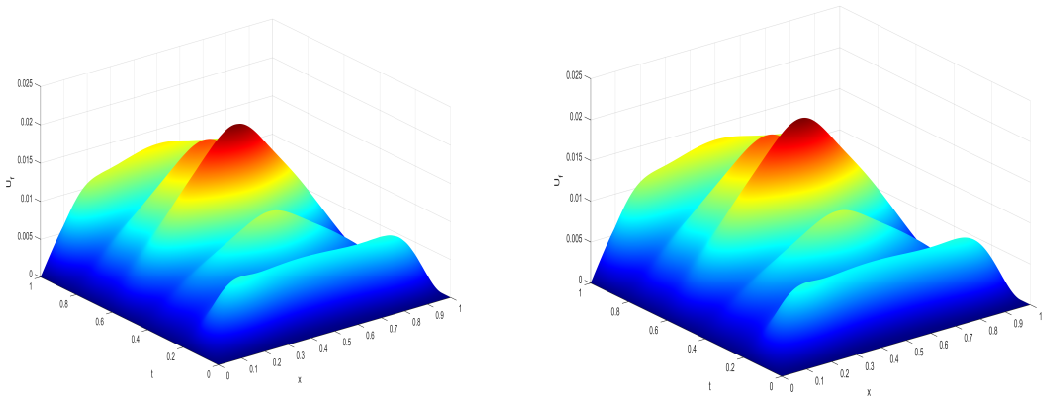

(a) $\tau = 1/120$ (b) $\tau = 1/1200$

Figure 1. Numerical solution U_f with different time step lengths and $h = 1/1200$.

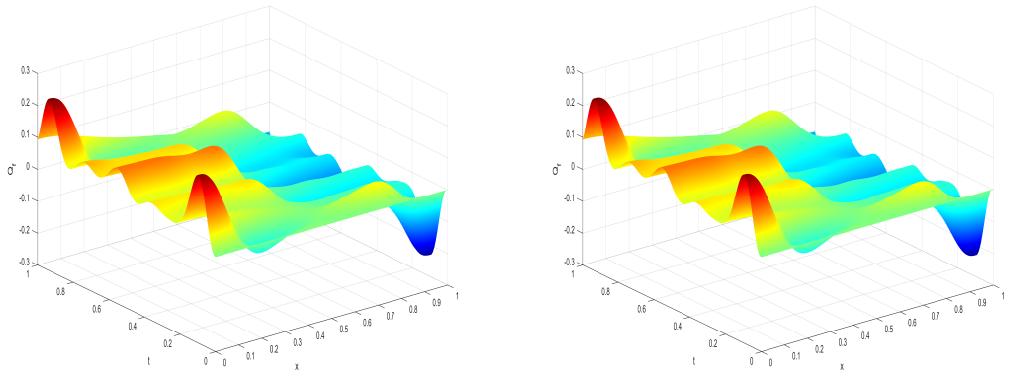

(a) $\tau = 1/120$ (b) $\tau = 1/1200$

Figure 2. Numerical solution Q_f with different time step lengths and $h = 1/1200$.

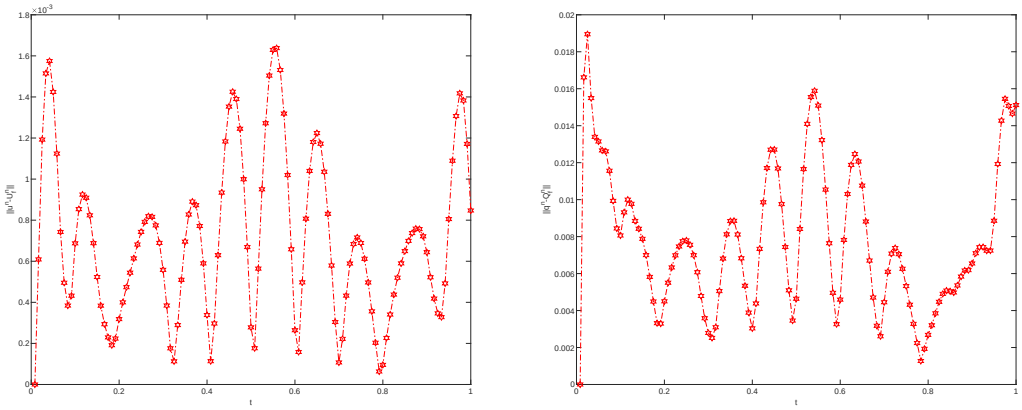

(a) $\|u^n - U_f^n\|$ (b) $\|q^n - Q_f^n\|$

Figure 3. L^2-errors at different time.

5.3. Example 3

For comparison and validation of feasibility, we still carry out the numerical calculation by taking Example 1. Here, we apply the linearized technique (2.16) to deal with the nonlinear term. One can see from the numerical results in Table 7 that the optimal spatial convergence data is almost consistent with the calculation results in Example 1, which uses the linearized method (2.17)(a). It indicates that the linearization technique adopted in this paper is feasible. Further, comparison of CPU time in Table 2 and Table 7 shows that computing time in this example is slightly slower, which may be caused due to the linearization for the $m-1$ layer.

Table 7. Spatial convergence results with $\tau = \frac{1}{10000}$ for TT-M MFE method (Example 3).

α	θ	h	$\|u-u_f\|$	rate	$\|q-q_f\|$	rate	CPU(s)
		1/200	4.5123E-05	-	6.9060E-04	-	82
	0.1	1/300	2.0078E-05	1.9971	3.0697E-04	1.9997	112
		1/400	1.1299E-05	1.9983	1.7268E-04	1.9998	174
		1/200	4.5124E-05	-	6.9060E-04	-	83
0.3	0.3	1/300	2.0079E-05	1.9971	3.0697E-04	1.9997	106
		1/400	1.1300E-05	1.9982	1.7268E-04	1.9998	169
		1/200	4.5125E-05	-	6.9060E-04	-	84
	0.5	1/300	2.0079E-05	1.9970	3.0697E-04	1.9997	113
		1/400	1.1301E-05	1.9982	1.7268E-04	1.9998	175
		1/200	4.5596E-05	-	1.1129E-03	-	87
	0.1	1/300	2.0282E-05	1.9979	4.9470E-04	1.9997	115
		1/400	1.1409E-05	1.9999	2.7828E-04	1.9998	184
		1/200	4.5597E-05	-	1.1130E-03	-	88
0.8	0.3	1/300	2.0283E-05	1.9978	4.9470E-04	1.9997	122
		1/400	1.1410E-05	1.9997	2.7828E-04	1.9998	180
		1/200	4.5599E-05	-	1.1130E-03	-	89
	0.5	1/300	2.0285E-05	1.9977	4.9470E-04	1.9997	113
		1/400	1.1412E-05	1.9996	2.7829E-04	1.9998	183
		1/200	4.5585E-05	-	1.3908E-03	-	89
	0.1	1/300	2.0273E-05	1.9985	6.1820E-04	1.9997	119
		1/400	1.1400E-05	2.0010	3.4776E-04	1.9998	180
		1/200	4.5587E-05	-	1.3908E-03	-	80
0.99	0.3	1/300	2.0274E-05	1.9984	6.1821E-04	1.9997	113
		1/400	1.1402E-05	2.0008	3.4776E-04	1.9998	177
		1/200	4.5588E-05	-	1.3908E-03	-	79
	0.5	1/300	2.0276E-05	1.9983	6.1821E-04	1.9997	120
		1/400	1.1403E-05	2.0006	3.4776E-04	1.9998	178

5.4. Example 4

Table 8. Temporal convergence results without correction parts with $h = \frac{1}{1000}$ (Example 4).

α	θ	τ	$\|u - U_f\|$	rate	$\|q - Q_f\|$	rate
		1/16	1.1815E-03	-	8.4390E-03	-
	0.1	1/25	5.8634E-04	1.5698	3.9830E-03	1.6824
		1/36	3.1749E-04	1.6823	2.2265E-03	1.5950
		1/49	1.8309E-04	1.7855	1.3153E-03	1.7072
		1/16	6.7319E-04	-	4.6262E-03	-
0.1	0.3	1/25	2.9762E-04	1.8289	2.1182E-03	1.7504
		1/36	1.5559E-04	1.7787	1.0860E-03	1.8322
		1/49	8.9665E-05	1.7877	6.1517E-04	1.8434
		1/16	7.5071E-05	-	2.2560E-04	-
	0.5	1/25	3.1201E-05	1.9673	6.4598E-05	2.8021
		1/36	1.5837E-05	1.8596	3.8075E-05	1.4497
		1/49	9.1062E-06	1.7950	2.8062E-05	0.9897
		1/16	1.1096E-03	-	8.4598E-03	-
	0.1	1/25	4.9205E-04	1.8221	4.0096E-03	1.6730
		1/36	2.5452E-04	1.8078	2.1919E-03	1.6562
		1/49	1.4087E-04	1.9187	1.2752E-03	1.7570
		1/16	6.4783E-04	-	4.7511E-03	-
0.3	0.3	1/25	2.7961E-04	1.8827	2.1137E-03	1.8149
		1/36	1.3972E-04	1.9025	1.0627E-03	1.8857
		1/49	7.6362E-05	1.9597	6.1178E-04	1.7911
		1/16	3.1590E-04	-	3.4312E-04	-
	0.5	1/25	1.2862E-04	2.0135	1.4706E-04	1.8985
		1/36	6.1578E-05	2.0199	7.4871E-05	1.8513
		1/49	3.2782E-05	2.0449	4.4690E-05	1.6738
		1/16	1.1653E-03	-	9.0917E-03	-
	0.1	1/25	4.9632E-04	1.9125	4.3197E-03	1.6675
		1/36	2.4321E-04	1.9562	2.3523E-03	1.6668
		1/49	1.3205E-04	1.9809	1.3680E-03	1.7581
		1/16	8.4052E-04	-	5.1034E-03	-
0.5	0.3	1/25	3.4388E-04	2.0026	2.2553E-03	1.8298
		1/36	1.6484E-04	2.0165	1.1321E-03	1.8901
		1/49	8.8163E-05	2.0298	6.5240E-04	1.7877
		1/16	7.4734E-04	-	4.1001E-04	-
	0.5	1/25	3.0590E-04	2.0016	1.8169E-04	1.8237
		1/36	1.4698E-04	2.0100	9.2128E-05	1.8624
		1/49	7.8605E-05	2.0301	5.1259E-05	1.9017

Table 9. Temporal convergence results by adding correction parts with $h = \frac{1}{1000}$ (Example 4).

α	θ	τ	$\|u - U_f\|$	rate	$\|q - Q_f\|$	rate
		1/16	3.0356E-04	-	1.7376E-03	-
	0.1	1/25	1.2169E-04	2.0482	7.1047E-04	2.0039
		1/36	5.7766E-05	2.0433	3.4171E-04	2.0073
		1/49	3.0527E-05	2.0687	1.8358E-04	2.0152
		1/16	7.5801E-04	-	3.6033E-03	-
0.1	0.3	1/25	2.9970E-04	2.0792	1.4975E-03	1.9675
		1/36	1.4141E-04	2.0598	7.3055E-04	1.9684
		1/49	7.4831E-05	2.0644	3.9721E-04	1.9764
		1/16	9.9172E-04	-	3.7014E-03	-
	0.5	1/25	3.8117E-04	2.1426	1.5811E-03	1.9060
		1/36	1.7754E-04	2.0953	7.8511E-04	1.9198
		1/49	9.3053E-05	2.0954	4.3188E-04	1.9386
		1/16	3.8731E-04	-	2.0865E-03	-
	0.1	1/25	1.5647E-04	2.0309	8.5231E-04	2.0061
		1/36	7.4130E-05	2.0487	4.0953E-04	2.0100
		1/49	3.9028E-05	2.0809	2.1954E-04	2.0222
		1/16	9.6616E-04	-	4.0215E-03	-
0.3	0.3	1/25	3.8454E-04	2.0643	1.6689E-03	1.9707
		1/36	1.8134E-04	2.0614	8.1646E-04	1.9606
		1/49	9.5941E-05	2.0650	4.4504E-04	1.9683
		1/16	1.2274E-03	-	3.7900E-03	-
	0.5	1/25	4.7871E-04	2.1097	1.6109E-03	1.9171
		1/36	2.2407E-04	2.0818	8.0161E-04	1.9140
		1/49	1.1774E-04	2.0871	4.4331E-04	1.9214
		1/16	4.8632E-04	-	2.5322E-03	-
	0.1	1/25	1.9796E-04	2.0139	1.0356E-03	2.0034
		1/36	9.4202E-05	2.0366	4.9789E-04	2.0085
		1/49	4.9830E-05	2.0656	2.6685E-04	2.0230
		1/16	1.1980E-03	-	4.4807E-03	-
0.5	0.3	1/25	4.8062E-04	2.0464	1.8632E-03	1.9662
		1/36	2.2775E-04	2.0481	9.1771E-04	1.9421
		1/49	1.2091E-04	2.0540	5.0351E-04	1.9470
		1/16	1.4738E-03	-	3.8871E-03	-
	0.5	1/25	5.8365E-04	2.0755	1.6369E-03	1.9379
		1/36	2.7457E-04	2.0680	8.1438E-04	1.9146
		1/49	1.4530E-04	2.0643	4.5316E-04	1.9014

In this example, we choose the solution $u = t^{2+\alpha}\sin(\pi x)$, which has weaker regularity with comparison to the case in Example 1. We choose the same space-time domain and the nonlinear term $g(u)$ as in

Example 1. We provide the source term f, which we omit here, such that the equation has the current exact solution u. For this case with weak regularity, we continue to apply the linearized technique (2.16) to deal with the nonlinear term.

By taking $\tau = 1/16, 1/25, 1/36, 1/49$, $\alpha = 0.1, 0.3, 0.5$, $\theta = 0.1, 0.3, 0.5$, and the fixed space step $h = 1/1000$, we implement numerical tests and obtain the numerical results shown in Table 8, from which one can see that most data cannot achieve second-order approximation results in time. For solving this issue, under the same parameters, we consider the corrected scheme with correction parts, and arrive at optimal time second-order convergence results listed in Table 9, which imply that the numerical scheme by adding the correction parts can effectively solve the problem of accuracy loss and restore the optimal convergence order. Further, based on the data from Tables 8–9, we show the case of the convergence rate in Figures 4–5 for U_f and Q_f, from which one can see intuitively, that with comparison to the case without adding the correction parts, the optimal convergence rate can be achieved by adding the correction parts.

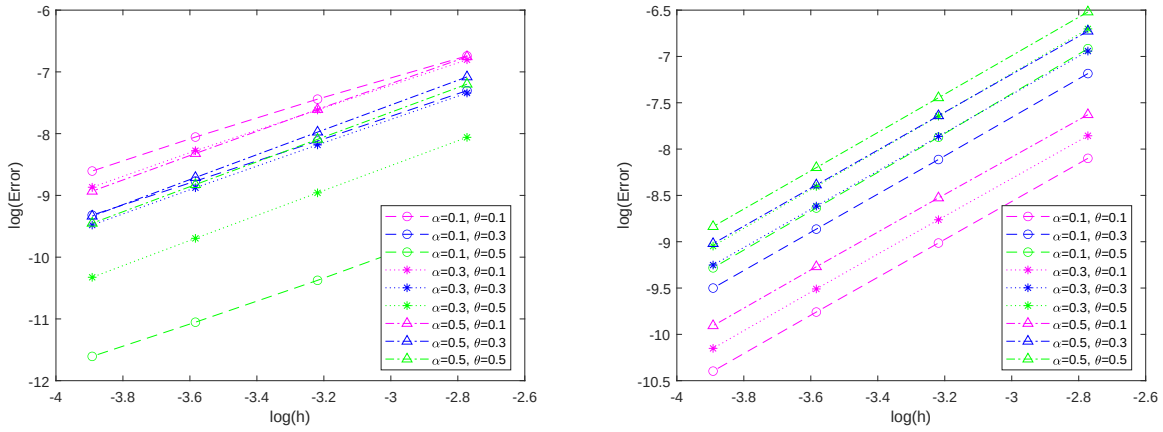

(a) The case without correction parts (b) The case with correction parts

Figure 4. Time convergence rates of U_f without or with correction parts.

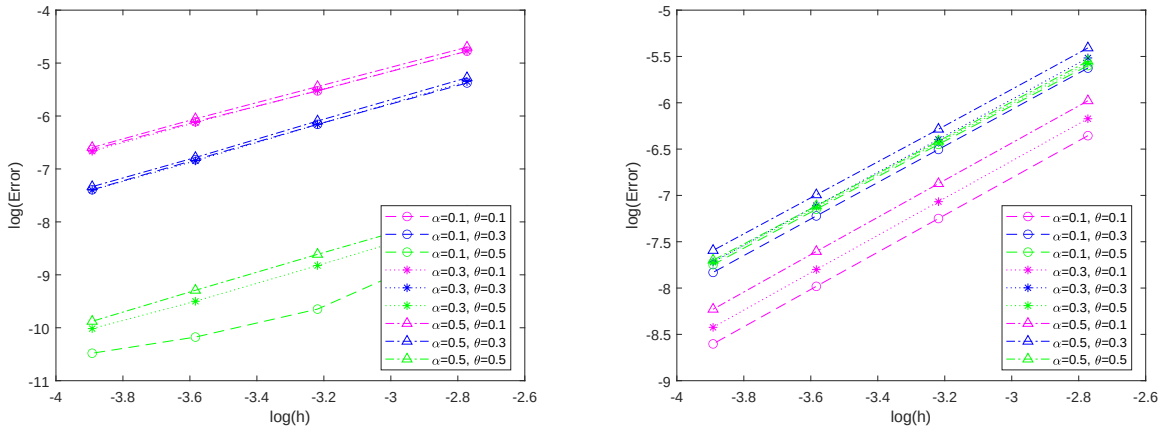

(a) The case without correction parts (b) The case with correction parts

Figure 5. Time convergence rates of Q_f without or with correction parts.

6. Conclusions and Advancements

In this article, we developed a fast TT-M MFE method for solving the nonlinear fractional hyperbolic wave model. We derived optimal a priori error results for the fully discrete TT-M MFE scheme. To verify the correctness of theoretical results and the computational efficiency of the algorithm, we implemented four numerical tests. For the cases with smooth solutions, one can see from the computing results that our TT-M MFE algorithm can obtain the similar convergence results as that computed by using the nonlinear MFE algorithm, while the computing time was reduced. Further, for the case with a weakly regular solution, the considered numerical scheme under certain parameters may lose computational accuracy. For handling this problem, we designed the corrected TT-M MFE method by adding the correction term to restore calculation accuracy.

In future works, we will design other TT-M MFE methods to solve some nonlinear fractional PDE models.

Acknowledgments

The authors would like to thank the editor and all the anonymous referees for their valuable comments, which greatly improved the presentation of the article. This work is supported by the National Natural Science Foundation of China (12061053, 12161063), Natural Science Foundation of Inner Mongolia (2022LHMS01004), Young innovative talents project of Grassland Talents Project, Program for Innovative Research Team in Universities of Inner Mongolia Autonomous Region (NMGIRT2413, NMGIRT2207).

Use of AI tools declaration

The authors declare they have not used Artificial Intelligence (AI) tools in the creation of this article.

Conflict of interest

The authors declare there is no conflict of interest.

References

1. S. W. Liu, H. Q. Wang, T. S. Li, Adaptive composite dynamic surface neural control for nonlinear fractional-order systems subject to delayed input, *ISA Trans.*, **134** (2023), 122–133. https://doi.org/10.1016/j.isatra.2022.07.027
2. Y. Li, H. Wang, X. Zhao, N. Xu, Event-triggered adaptive tracking control for uncertain fractional-order nonstrict-feedback nonlinear systems via command filtering, *Int. J. Robust Nonlinear Control*, **32** (2022), 7987–8011. https://doi.org/10.1002/rnc.6255
3. M. M. A. Khater, De Broglie waves and nuclear element interaction; Abundant waves structures of the nonlinear fractional Phi-four equation, *Chaos Solitons Fract.*, **163** (2022), 112549, https://doi.org/10.1016/j.chaos.2022.112549

4. M. M. A. Khater, R. A. M. Attia, Simulating the behavior of the population dynamics using the non-local fractional Chaffee-Infante equation, *Fractals*, 2023. https://doi.org/10.1142/S0218348X23402004
5. Y. Cao, B. L. Yin, Y. Liu, H. Li, Crank-Nicolson WSGI difference scheme with finite element method for multi-dimensional time fractional wave problem, *Comput. Appl. Math.*, **37** (2018), 5126–5145. https://doi.org/10.1007/s40314-018-0626-2
6. L. Feng, F. Liu, I. Turner, Finite difference/finite element method for a novel 2D multi-term time-fractional mixed sub-diffusion and diffusion-wave equation on convex domains, *Commun. Nonlinear Sci. Numer. Simulat.*, **70** (2019), 354–371. https://doi.org/10.1016/j.cnsns.2018.10.016
7. Y. Luchko, Fractional wave equation and damped waves, *J. Math. Phys.*, **54** (2013), 031505. https://doi.org/10.1063/1.4794076
8. B. L. Yin, Y. Liu, H. Li, F. H. Zeng, A class of efficient time-stepping methods for multiterm time-fractional reaction-diffusion-wave equations, *Appl. Numer. Math.*, **165** (2021), 56–82. https://doi.org/10.1016/j.apnum.2021.02.007
9. Z. G. Zhao, C. P. Li, Fractional difference/finite element approximations for the time-space fractional telegraph equation, *Appl. Math. Comput.*, **219** (2012), 2975–2988. https://doi.org/10.1016/j.amc.2012.09.022
10. J. H. Jia, X. C. Zheng, H. Wang, Numerical discretization and fast approximation of a variably distributed-order fractional wave equation, *ESAIM: Math. Model. Numer. Anal.*, **55** (2021), 2211–2232. https://doi.org/10.1051/m2an/2021045
11. H. R. Ren, Y. Liu, B. L. Yin, H. Li, Finite element algorithm with a second-order shifted composite numerical integral formula for a nonlinear time fractional wave equation, *Numer. Meth. Part. Differ. Equ.*, **40** (2024), e23066. https://doi.org/10.1002/num.23066
12. M. Li, C. M. Huang, Y. L. Zhao, Fast conservative numerical algorithm for the coupled fractional Klein-Gordon-Schrödinger equation, *Numer. Algor.*, **84** (2020), 1081–1119. https://doi.org/10.1007/s11075-019-00793-9
13. M. Li, M. F. Fei, N. Wang, C. M. Huang, A dissipation-preserving finite element method for nonlinear fractional wave equations on irregular convex domains, *Math. Comput. Simulat.*, **177** (2020), 404–419. https://doi.org/10.1016/j.matcom.2020.05.005
14. M. Li, Y. L. Zhao, A fast energy conserving finite element method for the nonlinear fractional Schrödinger equation with wave operator, *Appl. Math. Comput.*, **338** (2018), 758–773. https://doi.org/10.1016/j.amc.2018.06.010
15. M. H. Heydari, M. R. Hooshmandasl, F. M. Ghaini, C. Cattani, Wavelets method for the time fractional diffusion-wave equation, *Phys. Lett. A.*, **379** (2015) 71–76. https://doi.org/10.1016/j.physleta.2014.11.012
16. F. H. Zeng, Second-order stable finite difference schemes for the time-fractional diffusion-wave equation, *J. Sci. Comput.*, **65** (2015), 411–430. https://doi.org/10.1007/s10915-014-9966-2
17. A. Atangana, On the stability and convergence of the time-fractional variable order telegraph equation, *J. Comput. Phys.*, **293** (2015), 104–114. https://doi.org/10.1016/j.jcp.2014.12.043

18. M. H. Chen, W. H. Deng, A second-order accurate numerical method for the space-time tempered fractional diffusion-wave equation, *Appl. Math. Lett.*, **68** (2017), 87–93. https://doi.org/10.1016/j.aml.2016.12.010
19. H. F. Ding, A high-order numerical algorithm for two-dimensional time-space tempered fractional diffusion-wave equation, *Appl. Numer. Math.*, **135** (2019), 30–46. https://doi.org/10.1016/j.apnum.2018.08.005
20. Z. D. Luo, H. Wang, A highly efficient reduced-order extrapolated finite difference algorithm for time-space tempered fractional diffusion-wave equation, *Appl. Math. Lett.*, **102** (2020), 106090. https://doi.org/10.1016/j.aml.2019.106090
21. W. McLean, K. Mustapha, A second-order accurate numerical method for a fractional wave equation, *Numer. Math.*, **105** (2007), 481–510. https://doi.org/10.1007/s00211-006-0045-y
22. J. Ren, Z. Sun, Numerical algorithm with high spatial accuracy for the fractional diffusion-wave equation with Neumann boundary conditions, *J. Sci. Comput.*, **56** (2013), 381–408. https://doi.org/10.1007/s10915-012-9681-9
23. H. Sun, Z. Z. Sun, G. H. Gao, Some temporal second order difference schemes for fractional wave equations, *Numer. Meth. Part. Differ. Equ.*, **32** (2016), 970–1001. https://doi.org/10.1002/num.22038
24. M. Dehghan, M. Abbaszadeh, A. Mohebbi, Analysis of a meshless method for the time fractional diffusion-wave equation, *Numer. Algor.*, **73** (2016), 445–476. https://doi.org/10.1007/s11075-016-0103-1
25. G. Fairweather, X. H. Yang, D. Xu, H. X. Zhang, An ADI Crank-Nicolson orthogonal spline collocation method for the two-dimensional fractional diffusion-wave equation, *J. Sci. Comput.*, **65** (2015), 1217–1239. https://doi.org/10.1007/s10915-015-0003-x
26. Y. Yang, Y. Chen, Y. Huang, H. Wei, Spectral collocation method for the time-fractional diffusion-wave equation and convergence analysis, *Comput. Math. Appl.*, **73** (2017), 1218–1232. https://doi.org/10.1016/j.camwa.2016.08.017
27. M. M. A. Khater, D. C. Lu, Analytical versus numerical solutions of the nonlinear fractional time-space telegraph equation, *Modern Phys. Lett. B.*, **35** (2021), 2150324. https://doi.org/10.1142/S0217984921503243
28. M. M. A. Khater, K. S. Nisar, M. S. Mohamed, Numerical investigation for the fractional nonlinear space-time telegraph equation via the trigonometric Quintic B-spline scheme, *Math. Meth. Appl. Sci.*, **44** (2021), 4598–4606. https://doi.org/10.1002/mma.7052
29. W. Y. Tian, H. Zhou, W. H. Deng, A class of second order difference approximations for solving space fractional diffusion equations, *Math. Comput.*, **84** (2015), 1703–1727.
30. Z. B. Wang, S. W. Vong, Compact difference schemes for the modified anomalous fractional sub-diffusion equation and the fractional diffusion-wave equation, *J. Comput. Phys.*, **277** (2014), 1–15. https://doi.org/10.1016/j.jcp.2014.08.012
31. Y. Liu, Y. W. Du, H. Li, J. F. Wang, A two-grid finite element approximation for a nonlinear time-fractional Cable equation, *Nonlinear Dyn.*, **85** (2016), 2535–2548. https://doi.org/10.1007/s11071-016-2843-9

32. C. Li, S. Zhao, Efficient numerical schemes for fractional water wave models, *Comput. Math. Appl.*, **71** (2016), 238–254. https://doi.org/10.1016/j.camwa.2015.11.018
33. C. C. Ji, Z. Z. Sun, A high-order compact finite difference scheme for the fractional sub-diffusion equation, *J. Sci. Comput.*, **64** (2015), 959–985. https://doi.org/10.1007/s10915-014-9956-4
34. Y. Liu, M. Zhang, H. Li, J. C. Li, High-order local discontinuous Galerkin method combined with WSGD-approximation for a fractional subdiffusion equation, *Comput. Math. Appl.*, **73** (2017), 1298–1314. https://doi.org/10.1016/j.camwa.2016.08.015
35. Y. Liu, Y.W. Du, H. Li, F. Liu, Y.Wang, Some second-order θ schemes combined with finite element method for nonlinear fractional cable equation, *Numer. Algor.*, **80** (2019), 533–555. https://doi.org/10.1007/s11075-018-0496-0
36. A. K. Pani, An H^1-Galerkin mixed finite element method for parabolic partial differential equations, *SIAM J. Numer. Anal.*, **35** (1998), 712–727. https://doi.org/10.1137/S0036142995280808
37. Y. Liu, H. Li, H^1-Galerkin Mixed finite element methods for pseudo-hyperbolic equations, *Appl. Math. Comput.*, **212** (2009), 446–457. https://doi.org/10.1016/j.amc.2009.02.039
38. L. Guo, H. Z. Chen, H^1-Galerkin Mixed finite element method for the regularized long wave equation, *Computing*, **77** (2006), 205–221. https://doi.org/10.1007/s00607-005-0158-7
39. D. Y. Shi, J. J. Wang, F. Yan, Unconditional superconvergence analysis of an H^1-Galerkin mixed finite element method for nonlinear Sobolev equations, *Numer. Meth. Part. Differ. Equ.*, **34** (2018) 145–166. https://doi.org/10.1002/num.22189
40. Z. G. Shi, Y. M. Zhao, F. Liu, Y. F. Tang, F. L. Wang, Y. H. Shi, High accuracy analysis of an H^1-Galerkin mixed finite element method for two-dimensional time fractional diffusion equations, *Comput. Math. Appl.*, **74** (2017), 1903–1914. https://doi.org/10.1016/j.camwa.2017.06.057
41. C. Wen, Y. Liu, B. L. Yin, H. Li, J. F. Wang, Fast second-order time two-mesh mixed finite element method for a nonlinear distributed-order sub-diffusion model, *Numer. Algor.*, **88** (2021), 523–553. https://doi.org/10.1007/s11075-020-01048-8
42. Y. Liu, Z.D. Yu, H. Li, F. Liu, J. F. Wang, Time two-mesh algorithm combined with finite element method for time fractional water wave model, *Int. J. Heat Mass Transf.*, **120** (2018), 1132–1145. https://doi.org/10.1016/j.ijheatmasstransfer.2017.12.118
43. W. L. Qiu, D. Xu, J. Guo, J. Zou, A time two-grid algorithm based on finite difference method for the two-dimensional nonlinear time-fractional mobile/immobile transport model, *Numer. Algor.*, **85** (2020), 39–58. https://doi.org/10.1007/s11075-019-00801-y
44. Y. X. Niu, Y. Liu, H. Li, F. W. Liu, Fast high-order compact difference scheme for the nonlinear distributed-order fractional Sobolev model appearing in porous media, *Math. Comput. Simulat.*, **203** (2023), 387–407. https://doi.org/10.1016/j.matcom.2022.07.001
45. Z. C. Fang, J. Zhao, H. Li, Y. Liu, A fast time two-mesh finite volume element algorithm for the nonlinear time-fractional coupled diffusion model, *Numer. Algor.*, **93** (2023), 863–898. https://doi.org/10.1007/s11075-022-01444-2
46. B. Yin, Y. Liu, H. Li, S. He, Fast algorithm based on TT-M FE system for space fractional Allen-Cahn equations with smooth and non-smooth solution, *J. Comput. Phys.*, **379** (2019), 351–372. https://doi.org/10.1016/j.jcp.2018.12.004

47. Q. F. Li, Y. P. Chen, Y. Q. Huang, Y. Wang, Two-grid methods for nonlinear time fractional diffusion equations by L1-Galerkin FEM, *Math. Comput. Simulat.*, **185** (2021), 436–451. https://doi.org/10.1016/j.matcom.2020.12.033

48. O. Ladijzenskaia, The Mathematical Theory of Viscous Incompressible Fluid, *Gordon and Breach*, 1969.

49. E. Cuesta, C. Lubich, C. Palencia, Convolution quadrature time discretization of fractional diffusion-wave equations, *Math. Comp.*, **75** (2006), 673–696. https://doi.org/10.1090/s0025-5718-06-01788-1

50. F. H. Zeng, Z. Q. Zhang, G. E. Karniadakis, Second-order numerical methods for multi-term fractional differential equations: Smooth and non-smooth solutions, *Comput. Methods Appl. Mech. Engrg.*, **327** (2017), 478–502. https://doi.org/10.1016/j.cma.2017.08.029

51. B. Yin, Y. Liu, H. Li, A class of shifted high-order numerical methods for the fractional mobile/immobile transport equations, *Appl. Math. Comput.*, **368** (2020), 124799. https://doi.org/10.1016/j.amc.2019.124799

AIMS Press